NORWEGIAN UNIVERSITY OF SCIENCE AND TECHNOLOGY
NTNU

Future Operation and Control of Power Systems- Laboratory Models and Real-Time Simulation

by

Mesgena, Daniel Weldai

A thesis submitted in fulfillment for the
degree of Masters

in the

Faculty of Information Technology and Electrical Engineering
Department of Electric Power Engineering

June 2022

Declaration of Authorship

I, Daniel Weldai, declare that this thesis titled, 'Future Operation and Control of Power Systems- Laboratory Models and Real-Time Simulation ' and the work presented in it are my own. I confirm that:

- This work was done wholly or mainly while in candidature for a research degree at this University.
- Where any part of this thesis has previously been submitted for a degree or any other qualification at this University or any other institution, this has been clearly stated.
- Where I have consulted the published work of others, this is always clearly attributed.
- Where I have quoted from the work of others, the source is always given. With the exception of such quotations, this thesis is entirely my own work.
- I have acknowledged all main sources of help.
- Where the thesis is based on work done by myself jointly with others, I have made clear exactly what was done by others and what I have contributed myself.

Signed: Daniel

Date: 26.06.2022

"Those who walk with God, always reach their destination."

A smooth sea never made a skillful mariner !!

Abstract

Recently, growing electrical energy demand and increasing integration of renewable energy sources in power system have led to new challenges for the transmission system operators and on the network planning step. Thus, it is required to investigate and analyze properly the impacts of integrated RES on the power system. By connecting power sources like wind and solar to the grid using converters, there will be a significant impact on the performance and reliability of the electricity grid. This is largely because of the variability of renewable resources and lack of large-scale economical storage capability. At the same time the amount of high voltage direct current (HVDC) links connecting the Nordic power system to other grids is increasing. When importing power, this also contributes to imbalance power in the system. In addition, flexible load and increasing energy consumption have also problem in the stability of the power network. One way of controlling those sudden changes in the network is by real-time digital simulation and accurate dynamic load model. This is to provide a response at exact time to return the system in stability. In this thesis, a dynamic load model is developed and implemented in the Python Dynamic Power System Simulation (DynPSSimpy).

Real-time digital simulation is specially designed hardware and software integrated computer system used to study Electromagnetic Transient (EMT) Phenomena in power systems. As the name implies, it can perform power system simulations at computational speeds equal to real-time operation. However, modelling of detailed networks in RTS would require many hardware resources. The main goal of this thesis is to develop an equivalent dynamic load model for the stability analysis of the networks in RTS, which should not only enhance RTS's capability of simulating large power systems, but more importantly, improve the accuracy of model networks. The accuracy of dynamic load modelling plays a very important role in analyzing the stability systems. To respond for every event in the system with accurate injection or extraction of desired power to the network.

The system used in the study is the Nordic 44 model, which is an aggregated model of the Nordic power system. All simulations are performed in a static and dynamic power system simulation tool in Python script and dynamic load model, which are built using differential equations. In the future the Nordic power system supply will be dominated by renewable energy sources (RES) to achieve zero-carbon emissions, where the integration of wind and PV is increasing. At the same time, the demand side is more flexible due to new technology, such as electric vehicles, electrification of transport etc. Therefore, real-time simulation and accurate dynamic load models are the key to control the complex power system in real-time.

Acknowledgements

All praise is to the LORD, the most Merciful, the most Compassionate, the Creator of all that exist.

I have always seen myself as a man of faith and this faith has been one of the main driving forces in my adult life. The comfort and solace I find in God has given me the strength to pursue my goals and the peace of mind to overcome difficult times; His love makes everything possible.

I have never been a good writer; I always related more to numbers and equations than ever did to words, which is probably why I became an engineer. However, as I finish this chapter of my life, I would like to take a moment to express my appreciation and gratitude towards everyone who has helped or supported me in any way during this thesis.

The completion of this thesis has required an enormous amount of work and effort from my part; however none of it would have been possible without the support and guidance from Professor Kjetil Uhlen, for his continuous counseling through the last year, and for helping me with both the project work and this thesis. His knowledge on the topic, and constructive feedback has been essential for my work. I would also like to thank doctoral student Hallvar Haugdal, for letting me use his dynamic power system simulation program. Furthermore, I would like to appreciate the excellent support of Pål Erikson. He took his time to review my work and gave very helpful feedback's that helped me maintain focus.

Most especially, my profound gratitude goes to my family, for their support throughout my academic journey so far. My families were always there for me when I felt lonely away from home. I love you more than you can imagine. In particular I am grateful to my brother, Asmerom Weldai, for his continuous support. Your advice, encouragement, principles, and extraordinary motivations helped me aspire to be the best I can possibly be in life. I would not be where I am without you!

No man's life is complete without friends; as a kid I grew up surrounded by a small group of friends and along the way I was lucky enough to be able to keep them and meet new persons whom now I am proud to call my friends. The following names are meant to be a small recognition to the persons I consider true friends and whose support has helped me get where I am now: Bereket Tesfamariam, Sirak Hagos, Bereket Russom, Yohannes Solomon, Tesfealem Haile, Meron Fissihasion, Merihawi Amanuel and Daniel Berhe.

Contents

List of Figures

List of Tables

Abbreviations

RES	**R**enewable **E**nergy **S**ource
HVDC	**H**igh **V**oltage **D**irect **C**urrent
TNA	**T**ransient **N**etwork **A**nalayses
EMT	**E**Electro **M**agnetic **T**ransient
EMTP	**E**lectro- **M**agnetic **T**ransient **P**rogram
ATL	**A**rtificial **T**ransmission **L**ine
RTS	**R**eal **T**ime **S**imulation
PV	**P**hoto **V**oltaic
TSO	**T**ransmission **S**ystem **O**perator
DSO	**D**istribution **S**ystem **O**perator
DTS	**D**ispatcher **T**raining **S**imulation
RCP	**R**apid **C**ontrol **P**rototyping
HIP	**H**ardware-**I**n-the- **L**oop
RBS	**R**apid **B**atch **S**imulation
RTW	**R**eal **T**ime **W**orkshop
RTWT	**R**eal **T**ime **W**indow **T**arget
SCADA	**S**ystem **C**ontrol **A**nd **D**ata **A**cquisition
DSP	**D**igital **S**ignal **P**rocessing
COTS	**C**ommercial **O**ff- **T**he- **S**heft
FPGA	**F**ield **P**rogrammable **G**ate **A**rray
AI	**A**rtificial **I**ntelligence
SIL	**S**oftware- **I**n-the- **L**oop
DT	**D**igital **T**win
NASA	**N**ational **A**eronautics and **S**pace **A**dministration
ZIP	**Z**-constant Impedance **I**current **P**-Power

LED	**L**ight **E**mitted **D**iode
PMU	**P**hasor **M**easurement **U**nit
IM	**I**nduction **M**otor
CPL	**C**onstant **P**ower **L**oad
CRL	**C**onstant **R**esistive **L**oad
CCL	**C**onstant **C**urrent **L**oad
GUI	**G**raphical **U**ser **I**nterface
DEA	**Differential- A**lgebraic **E**quations
ODE	**O**rdinary **D**ifferntial **E**quation
DynPSSimpy	**D**ynamic **P**ower **S**ystem **S**imulation **P**ython
CCT	**C**ritical **C**learing **T**ime
PTP	**P**recision **T**ime **P**rotocol
GPS	**G**lobal **P**ositioning **S**ystem
PDC	**P**hasor **D**ata**C**oncentrator

Dedicate to my family.

Chapter 1

Introduction

Since the turn of the century, power system stability has been recognized as a demanding concern for secure system operation. Many major blackouts caused due to power system instability have illustrated the importance of voltage stability [1]. For many decades, the utilities have been the primary concern for angle instability. However, in the last two decades power systems have operated under much more stressed conditions than they usually had in the past. There are number of factors responsible for this, such as continuing growth in interconnections, the use of new technologies, bulk power transmissions over long transmission lines and environmental pressures on transmission expansion. Other examples are increased electricity consumption in heavy load areas, new system loading patterns due to the opening up of the electricity market, growing use of induction machines and large penetration of wind generators and local uncoordinated controls in systems. Under these stressed conditions a power system can exhibit a new type of unstable behaviour, namely, voltage instability. Therefore, in recent years, voltage stability has become a major research area in the field of power systems after a number of voltage instability incidents were experienced around the world.

The power system consists of a power plant, substations, transmission and distribution network and electric power load. Models of generator, transformer and electrical grid have made significant progress, while the load model is comparatively the most challenging because of its diversity and stochastic behavior. Power system modelling was long mostly focused on accurately representing generation and transmission, whereas load modelling did not develop at the same pace [2]. The credibility of power system simulation was significantly reduced by the discrepancy between stringent generator, transformer, and transmission network models and imprecise load models. Furthermore, the contribution of the renewable energy resources and flexible load has greatly increased the stability of the power system. Therefore, load modeling is the process

to ensure model structure and parameters according to electric power response to the change of load bus voltage and frequency.

1.1 Background and Motivation

According to Andrei [3], the power system is frequently recognized as the largest and most complicated human invention. It consists of numerous equipments like power transformers, synchronous generators, cables, capacitor banks, transmission lines, power electronic devices, thousands of buses etc. Those equipments enable safe and efficient generation, transmission and delivery of power to local and remote areas. As a result of this complexity, it is crucial to conduct various assessments of potential disturbances to make sure the system is reliable and maintain a state of stability. However, due to the continuous operation of power system and the high cost of equipment, most researchers are developing computer programs designed for simulations of the real system such that safety of the equipment and human interaction is not compromised. However, simulation of power system helps network operators and planners to forecast possible disturbances, provides adequate protection schemes and aids realistic future grid expansion.

As stated in [4], it is proposed that power system simulation is a critical element in power system planning and operation. The simulation results depend to a great extent on models of the system components, e.g, models of generator, excitation systems, transformers, lines, loads, capacitor banks, and other related equipment. One of the most challenging element to model in a power system is the system load, due to its diversity and complexity. Understanding the load is specially crucial when power systems are operated close to their stability limits. The load comprehends the devices in a power system that consume electrical energy, for instance, motors, lamps, office equipment, home appliances and so on. A common practice among Transmission System Operators (TSO) and Distribution System Operators (DSO) is to represent the loads with the aggregated models, as it would be unrealistic to represent every power consuming device in detail in such large systems [5].

Nowadays, the power system network has became more and more complicated due to the integration of renewable generation and new types of load [6]. The power generated by wind turbines and solar panels is a fluctuating variable. Modern non-linear power electronic loads, such as electric automobiles and transport electrification, are among the new forms of loads that are now accounting for a major portion of the total load. Due to more variable, renewable power generation and flexible demands, the Nordic TSOs foresee increasing challenges in the operation of the power system in future. In order to better analyze the power system stability, it is necessary to build accurate dynamic load model with correct parameters. However, the number of load model parameters is proportional to the size of the power system. Therefore, for a large power system, it is required a significant amount of human and financial resources to develop accurate load model parameters for every bus in the system. Among these load model parameters,

some may have a significant influence on the power system stability, while others may have an influence that can be neglected. Therefore, only the important parameters need to be modelled accurately and the level of accuracy of simulation will not be affected.

The contribution of flexible load and renewable energy sources has significantly expanded the power system network over the past decades. Recent reports suggest that the nations like Germany and the Nordic nations have covered a substantial amount of their energy requirements completely through the use of renewable energy sources. Consequently several technical challenges are being faced by utilities with respect to planning and operations of the modern power system, as highlighted in [7]. Due to the deployment of renewable energy sources and reduced carbon emissions, the structure of the modern power system is becoming increasingly complicated. These challenges are mainly attributed to high penetration of RES in the grid sections that have low demands. However, such situations have led to numerous efforts on research that investigates the influence of high influx of power electronic components in power systems. The major challenge of large scale integration of RES, especially at the distribution system level, is their behaviour and response to faults and other disturbances that might occur in the transmission system.

Despite the fact that the network of the power system gradually becomes ever more complex. At the same time, modern technology offers us new opportunities to monitor and predict the state of the network in real-time, and the ability to initiate automatic response to stabilize critical parameters to avoid system collapse. Thus, accurate dynamic load model and real-time simulation are the main important tools in this thesis to prevent the system from hazardous blackout.

1.2 Literature Review

When a power system engineer is required to investigate complex power system phenomena, simulation is one of the most effective methods at their disposal. For quicker and more accurate results, the power system community has recently concentrated mostly on dynamic power grid simulations or transient stability analysis, as explained in [8]. Simulation of power system dynamics is defined as an old bread-and-butter technology in power system engineering. There are many distinct simulation tools, including transient network analyses (TNA), artificial transmission line(ATL), analogue simulator, electromagnetic transients program (EMTP), transient stability analysis and long term dynamic simulation program, dispatcher training simulator (DTS), etc [9]. Over the past few decades, feed in from renewable energy sources has increased while at the same time more and more thermal generation units have been shuttered. As a result, ensuring a secure and reliable operation of power systems has been a challenging task. Real-time simulation tools are a robust and practical way to face these challenges. In addition, real-time simulation tools offer the computational speed advantage and allow studying a very large number of operational scenarios in less time. Moreover, such tools can provide real-time synchronized simulations and allow interfacing with external physical devices, which can be used to validate physical controllers, improve designs and even develop models [10].

In power system stability studies, the models of generators, and the characteristics of the loads are important variables influencing system stability [9]. Prior to two decades ago, representation of the generating unit received the majority of focus in power performance, whereas that of the loads received only a minor amount of attention. However, the load subsystem shows a significant impact on the performance of the power system even if they are static loads. This is due to the loads' active and reactive power dependencies on the system's voltage and frequency. Therefore, improvement of power system stability studies requires a careful consideration of the load types and their appropriate modelling. This is of special importance due to the widespread use of new power generation and power electronics technologies in the power system[11]. Therefore, the representation of the effective power demand at the high voltage buses is necessary. Typically, this also takes into account the aggregate effect of numerous static and dynamic load devices. Furthermore, modern power systems also implement a number of control mechanisms and technologies to ensure the system is controlled and operated safely.

The Nordic power system , as represented by the TSOs in 2018, has a mixture of energy sources, with hydro, nuclear, and wind power being the main sources. this is described in article [12]. It comprises the interconnected power systems of Norway, Sweden, Finland

and parts of Denmark. Also, the Nordic region has many energy intensive industries and a large share of electricity heated houses. In fact, the electricity consumption and electricity's share of total power used here in Nordic region is higher than that of the rest of the EU. As well as development of electricity consumption is highly influenced by the weather during the year, with lower electricity demand in summer and increased consumption in wintertime. In addition, the uncertainty and variability of wind and solar generation can pose challenges for the grid operators. Variability in generation sources can require additional actions to balance the system [13]. Greater flexibility in the system may be needed to accommodate supply-side variability and the relationship between generation levels and loads. Sometimes wind generation will increase as load increases, but in cases in which renewable generation increases when load levels fall (or vice versa), additional actions to balance the system are needed. Another challenge occurs when wind and solar generation is available during low load levels. In some cases conventional generators may need to turn down to their minimum generation levels [13]. The result is a power system with new properties and challenges. These challenges are identified and described in [5], where they conclude that the main challenges in the period leading up to 2025 are meeting the demand for flexibility, ensuring adequate transmission and generation capacity to guarantee security of supply. In addition to meet the demand of the market, maintaining a good frequency quality and sufficient inertia in the system to ensure operational security.

1.3 Objectives of this Thesis

The main objectives of this thesis are real-time simulation control for a dynamic load model after interconnection of advanced technologies. At the same time, dynamic load model is needed for several purposes, where I want to study load control and model the power electronic loads. The particular items are as follows:

1. Identify and simulate a real-time flexible load model and observe the changes in the power network.
2. Design the load model, where I should be able to represent different kind of loads that have dynamic response and be able to represent flexible loads.
3. Develop a realistic load model of the system in Python DynPSSimPy and test the controls designed within real-time simulation.

1.4 Thesis Organization

This chapter gives a general synopsis of the purpose of this thesis. Chapter 2 presents fundamental concepts regarding real-time simulation and evolution of digital real-time simulation, as well as a brief explanation on the Digital Twin. In chapter 3, the first section describes existing load modelling methodologies, whereas the second section is about the identification of load model parameters and the last section explains how the the dynamic load model is implemented in laboratory model. Relevant results from this investigation are analysed and presented in chapter 4. Lastly, chapter 5 presents the conclusions derived from the performed analyses as well as suggestions for further research.

Chapter 2

Real-Time Simulation

2.1 Introduction

Numerous improvements in computational and simulation tools have led to tremendous progress in the field of designing, testing and analysing technologies[14]. In addition to those improvements, with the advent of computers and various easily accessible software packages, computer aided teaching tools have become an essential part of both the classroom lectures and laboratory experiments in any kind of education curriculum. It has been investigated by many researchers. In order to plan and develop electrical systems, simulators have been widely used for many years. The development of a broad range of applications, from aerospace to domestic appliances, has been significantly assisted by simulation, from the architecture of transmission lines in large-scale power systems to the optimization of motor drives in transportation.

For the last three decades, the evolution of simulation tools have been driven by the rapid evolution of computing technologies[15]. Computer technologies have rapidly increased in performance and spread extensively at constantly falling prices. Consequently, simulation tools have likewise experienced notable performance improvements and consistent cost reductions. This, in turn, has lead to the emergence of highly sophisticated simulation software applications that not only enable high-fidelity simulation of dynamic systems and related controls, but also automatic code generation for implementation in industrial controllers. In addition, high-performance simulation tools were previously out of range for all but the largest manufactures and utilities are now available to academics and engineers at reasonable prices.

This thesis introduces the role and the benefits of using real-time simulation in electrical system with a focus of electromagnetic transient (EMT), power system modeling,

and simulation, and control prototyping techniques. It also discusses the technological aspects and the concept of contemporary real-time digital simulators. In addition, I will describe the recent evolution of real-time simulators and define the digital twin with improvements and challenges in electric power system.

2.1.1 What is Real-Time Simulation

Based on the American Heritage Dictionary of the English language definition of a simulation, which is a representation of the operation or features of a system through the use or operation of another media. " Real-time simulation of the electric power system is the reproduction of output (voltage or currents) waveform, with the desire accuracy, that are representative of the behavior of the real power system being modeled". To achieve such a goal, a digital real-time simulator needs to solve the model equations for one time-step within the same time in real-world clock[16]. This is commonly known as fixed time-step simulation. It is important to note that other techniques exist that use variable time-steps. Such techniques are used for solving high frequency dynamics and non-linear systems, but are unsuitable for real-time simulation. To obtain mathematical expressions at a given time-step, each variable or system state is computed successively as a function of variables and stated at the end of the proceeding time-step.

In both *Belanger's* articles [14, 16], discrete-time simulations were investigated. The amount of real-time required to compute all equations and functions representing a system during a given time-step may be slower or faster than the duration of the simulation time-step as predicted in Figure 2.1 and Figure 2.2. As shown in Figure 2.1, the computing time is shorter than the fixed time-step (also referred to as accelerated simulation) while in Figure 2.2 the computing time is longer. These two situations are referred to as offline simulation. In both cases, the moment at which a result becomes available is irrelevant. Typically, when performing offline simulation, the objective is to obtain results as fast as possible. The system solving speed depends on available computation power and the system's mathematical model complexity.

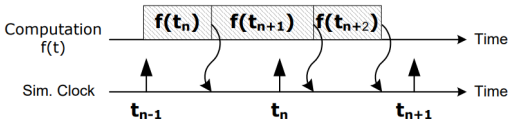

FIGURE 2.1: Offline simulation: Faster than real-time

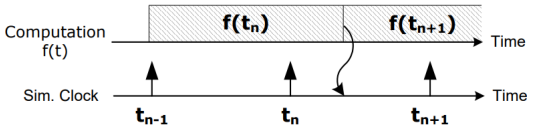

FIGURE 2.2: Offline simulation: slower than real-time

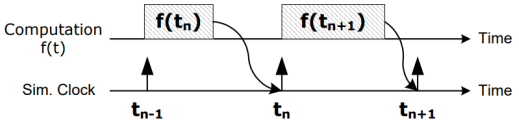

FIGURE 2.3: real-time simulation: Synchronized

Conversely, in real-time simulation, computation accuracy depends not only on a correct dynamic representation of the system but also on how long it takes to provide results, as shown in Figure 2.3. For a real-time simulation to be valid, the real-time simulator used must accurately produce the internal variables and outputs of the simulation within the same length of time that its physical counterpart would [15]. In fact, the time required to compute the solution at a given time step must be shorter than the wall clock duration of the time-step. This permits the real-time simulator to perform all operations necessary to make a real-time simulation relevant, including driving inputs and outputs to and from externally connected devices. For a given time-step, any idle-time preceding or following simulator operations is lost, whereas opposed to accelerated simulation, where idle time is used to compute the equations at the next time-step. In such a case, the simulator waits until the clock ticks to the next time-step. However, if the simulator operations are not at all achieved within the required fixed time-step, the real-time simulation is considered erroneous. This is commonly known as an "overrun". Based on these basic definitions, it can be concluded that a real-time simulator is performing as expected if the equations and states of the simulated system are solved accurately, with an acceptable resemblance to its physical counterpart, without the occurrence of overruns.

According to articles [14][15], digital real-time simulation is based on discrete time-steps in which the simulator solves model equations successively. To appropriately represent the frequency response of the system up to the quickest transient of interest, the appropriate time-step duration must be established. When the simulator achieves real-time without overruns, simulation results can be verified. Every time-step, the simulator

executes the same series of operations: first, read inputs and produce outputs; second, solve model equation; then, exchange results with other simulation nodes, and at last, wait for the beginning of the subsequent step. A simplified explanation of this routine suggests that the states of any externally connected device is sampled once at the beginning of each simulation time-step. Consequently, the state of the simulated system is communicated to external devices only once per time-step. Overruns happen when difference between the simulator results and their physical counterparts responses are seen when some of the real-time simulation timing constraints are not met.

Other research, [16], has examined the use of real-time simulation in engineering fields for a variety of purposes, such as Rapid Control Prototyping (RCP), Hardware-in-the-Loop testing (HIL), Rapid Batch Simulation (RBS) and others. Take into account a regulated process, which consists of a plant that is being acted upon by a controller. For instance in RCP applications, an engineer will use a real-time simulator to quickly implement a controller and connect it to the real plant. While HIL acts in an opposite manner, it refers to the condition where parts of the fully digital real-time simulation have been replaced with actual physical components. Its main purpose is to test actual controllers connected to a simulated plant. Of course, it is crucial to remember that human beings are the main role in the category of controllers. Hence, HIL simulation combines a simulated system with the actual hardware. For instance, a software simulation of the system plant is augmented with actuators and sensors from the designed system, while RBS is typically used to accelerate simulation in massive batch run tests. Since the real-time simulator operates in real-time, it continuously outputs data that accurately depicts the state of real system. A real-time simulator also allows the user to test actual hardware. Therefore, it is of great importance to understand the features and roles of the advanced simulator technologies [17].

Power electronic systems, electric drives, and their controls have become increasingly complicated over time, and they are now used more and more frequently across all industries, including power system networks, commercial, residential, and industrial electronics [18]. Real-time simulations are utilized extensively in many technical disciplines, including industry, education, and research organisations, thanks to development of software tools like MATLAB/SIMULINK with its Real-Time Workshop (RTW) and Real-Time Windows Target (RTWT). The progress of real-time simulation from analogue to fully digital is discussed in the following section.

2.2 Evolution of Digital-RTS

It was suggested in the article [19] that simulators have been extensively used in the planning and design of transmission system for decades. From physical and analogue simulators (HVDC simulators, TNA's) for electromagnetic transients and protection and control studies have given way to hybrid TNA and analogue digital simulators that can investigate electromechanical transient behavior, as well as completely digital real-time simulators.

In order to imitate certain elements of a physical system, amplifiers, resistors, capacitors, diodes were utilized in the 1960s. The physical connections between the TNA and HVDC simulators base are made in a way that reflects the real system [14][18]. This type of simulators has benefit of creating a close link between physical simulators and actual system parts. This feature enables system engineers to construct the simulation by mapping with the parameters ofĉomponents of the target physical systems while putting the least amount of work into mapping and translation [20]. However, users of physical simulation often struggle to solve those issues related to the computer rather than the simulation as a technique. For instance, users for physical simulation need to scale all the equations (differential equations) and shall grasp the necessary and often advanced solution, which implies transforming those equations from the problem domain into the physical component of the computer.

Whilst digital simulations imitate the physical system of the goal through mathematical representation. For these software-based simulations, methods were developed as early as 1969 and employed in certain well-known systems, reference article [18]. However, these early digital simulators work in a non-real-time manner as opposed to their analog counterparts, which may operate in real-time. As previously mentioned, real-time operation requires that a simulator must simulate an event that occurs in a physical system in less than one second. Unfortunately in the early digital simulators, those computations necessary to solve the required mathematical equations might take many seconds or even minutes rather than within one second to meet the real-time simulation requirement. With the quick development of micro-process, digital signal processing (DSP), together with improvement of software modelling techniques digital real-time simulators started to replace its physical counterparts in 1980s [16].

Digital real-time simulation researchers have employed relatively fast computers to accomplish real-time operation for short period of time, although these simulators are limited to rather simple systems [15]. The fundamental problem with these simulators is their scalability. The number of equations to solve increases as the represented system grows more realistic and sophisticated. Similarly, the number of computations that

must be done limits the applicability of these simulators. many digital signal processors can work in parallel to share the computing efforts required to solve the underlying equations in the simulation models to accomplish real-time operations for digital simulators. This DSP-based real-time simulators are developed with proprietary hardware and are commercially accessible. Because proprietary hardware limits its usefulness, certain alternative digital real-time simulators based on commercial supercomputers are developed, such as HYPERSIM [21] from Hyrdo-Quebec DO. Other attempts to run real-time simulations on low-cost ordinary PCs have been expedited by the introduction of low-cost Commercial Off-The-Shelf (COTS) multi-core processors. COTS enabled digital simulators can do complicated parallel simulations while lowering reliance on the inter-computer communications, and they are commonly used to model large-scale microgrids, aircraft and power system, according to [16]. The lack of efficiency, low-cost inter-computer communication lines made such advancement extremely challenging. Conversely, the advent of low-cost, readily accessible multi-core processors [22] from INTEL and AMD, and related COTS computer components have directly resolved the problem, creating opportunities for the establishment of significantly lower cost and easily scaled real-time simulators.

In source [23] it is highlighted that COTS-based high-end real-time simulators equipped with multi-core processor have been used in aerospace, robotics, automotive and power electronic system design and testing for a number of years. Such simulators are currently available to simulate EMT in large-scale power grids, micro-grids, wind farms and power systems installed all-electric ships and aircraft. These simulators, which can run on Windows, LINUX and standard real-time operating systems, have the potential to be compatible with a wide range of commercially available power system analysis software tools, such as PSS/E, EMTP-RV and PSCAD, as well as multi-domain software tools like SIMULINK and DYMOLA. The integration of multi-domain simulation tools with electrical simulators allows for the investigation of interactions between electrical, power electronic, mechanical and other systems.

In article [24] it was described that today's advancement in real-time simulation lies in running simulation models directly on Field-Programmable Gate Array (FPGAs) and graphics processing unit (GPU). FPGA and GPU are gaining foundation as a computation hardware for real-time simulation. This relatively new trend allows full utilization of the parallel nature of FPGAs so that the time-step for the real-time simulation can be set to very small and complicated system can be simulated by many small models [24][22]. Because of the parallel nature of FPGAs, calculation time inside each time-step is practically independent of system size in this simulator. Besides, once the model is running and the temporal constraints are fulfilled, overruns are not possible. Finally, and most critically, the simulation time-step can be very small, in the range of 250

nanoseconds. Model size is still limited since the number of gates in FPGAs is limited. However, this method has interesting prospects for investigation in the field of real-time power system simulation. Recently, PMU technology has been used to the power system, allowing to detection of line-outages using PMU real-time data.

Although it was stated in source [25] that real-time digital simulators are extremely advantageous when actual power system equipment are to be involved in the test program or research. This is referred to as a closed loop testing method [26], which represents an accurate and detailed way to evaluate the performance of the physical device(s) under actual operating conditions prior to their installation in the real network. The simulator can correctly simulated the response of the power system to the operation of the device under investigation, in addition to analyzing the performance of the real device.

2.3 Real-Time Simulation Techniques

Real-time simulation is an innovation of power semiconductors that plays an essential part in the simplification of electric power components. Simultaneously, advances in digital controllers such as Microprocessor, Digital Signal Processors (DSP) [27], Field Programmable Gate Array (FPGA),dSPACE and other Artificial Intelligence (AI) such as Fuzzy and Neural, can now be implemented for real-time applications [28]. For a long time, system validation was accomplished by non-real-time simulation of the concept early in the design process, followed by testing the system once the design was implemented. This approach has two significant drawbacks. First, the leap in the design process, from off-line simulation to real prototype is so large that it is prone to various issued and challenges associated to the simultaneous integration of several modules. Second, for any somewhat complicated system, the off-line, non-real-time simulation may become tediously long, particularly for electrical machine drives with switching power electronics.

There are various techniques that can be used for real-time control and simulation of electrical machines and drives. Several examples of this are Rapid Control Prototyping (RCP), Hardware-in-the -Loop (HIL) and Software-in-the-loop (SIL), and so on. Real-time simulators are commonly used in three types of applications [15]. In RCP applications, for instance, a plant controller is implemented using a real-time simulator and is connected to an actual plant. RCP provides various advantages over implementing an actual controller prototype. A controller prototype developed using a real-time simulator is more adaptable, quicker to implement and simpler to troubleshoot. In HIL applications, a physical controller is connected to a virtual plant running on a real-time simulator, rather than an actual plant. A minor modification to HIL and implementation of a controller using RCP is connected to a virtual plant through HIL. In addition to the advantages of RCP, HIL allows for early controller testing when physical test benches are unavailable.

Software-in-loop (SIL) [29] is another technique to represent, which represents the third logical step beyond the combination of RCP and HIL. With a sophisticated simulator, both controller and plant can be simulated in real-time in the same simulator. Unlike RCP and HIL, SIL does not employ inputs and outputs, preserving signal integrity. Besides, since both the controller and plant models are operated on the same simulator, synchronizing with the outside world is no longer a concern. It may be slower or faster than the real-time without affecting the validity of the results, making SIL excellent for accelerated simulation. In accelerated mode, a simulation runs quicker than real-time, enabling for a high number of tests to be done in short amount of time. As a result, SIL is highly suited for statically testing, such as Monte-Carlo simulations. SIL can

also run at slower rate than real-time. In this situation, if the real-time simulator lacks computational capability to approach real-time, a simulation may still be executed at a fraction of real-time, generally quicker than on a desktop computer.

2.3.1 Hardware-In-the-Loop Technique

The importance and evolution of the simulation were described in the preceding section. In general, a successful real-time simulation platform must have two key characteristics, fixed-step real-time processing and user-friendly interface to real hardware. Therefore fixed-step real-time operating systems such as QNX/Neutrino take the lead. Allowing real hardware to be in the simulation loop to communicate and exchange data with computing software in real time makes it possible to validate the design performance in a close-to real testing environment, which constitutes the so-called Hardware-in-the-Loop (HIL) simulation

[30]. As previously stated, HIL is an essential technique which is now used as a standard test and functional evaluation technology for control systems. It is widely used in automotive, aerospace and power generating and distribution industries [31]. HIL simulation entails incorporating actual physical hardware, most commonly a test controller or collection of distributed and networked controllers, but also real loads or other components, into a closed-loop real-time simulation of the plant. The simulated plant generates feedback and monitoring signals for the control systems in real-time, and the controllers respond by delivering control outputs and fault indicators back to the simulated plant. Thus, controller functionality can be tested and validated without putting safety or equipment at risk. In addition, fault conditions that are difficult to established in actual operation can be simulated, allowing controller responses to such conditions to be assessed. To give accurate controller responses, the simulation must precisely imitate the dynamic behavior of the plant, and the plant model must be performed in real-time with an adequate integration time-step. The integration time-step, which is dictated by the stability requirements of the highest frequency component, must be carefully set since it must be short enough to assure numerical accuracy yet large enough to allow all model calculations to be completed within it. For accurate simulation of complex electrical systems, step-sizes in the 10 to 30 milliseconds range are recommended to obtain acceptable accuracy for transients with frequency components from 3KHz to 10KHz [31].

An HIL simulations can help reduce development cycles and risk during RD, as well as lower total cost, and thoroughly test a subsystem before incorporating it into the system. Furthermore, increased system reliability by through extensive fault testing, better

system performance through optimum tuning under a range of operating situations, and increased service efficiency through commissioning and troubleshooting training. Moreover, when a given decision is exceedingly difficult to represent, it is more practical to utilize it directly in simulations than for modeling it [32].

2.4 Digital Twin

In [33] defined a phrase digital twin, which signifies digital transformation featuring a variety of sophisticated technologies such as machine learning and the Internet of Things. One such technology that recently gained visibility is the concept of the digital twin. This thesis will introduce digital twin, outline their idea, and discuss the advantages of implementing them in future power systems. The term digital twin was first introduced by Grieves in 2002 as a new concept in product life cycle management. Although it was first referred to as Mirrored Space Models in 2003, the concept subsequently evolved into information mirroring models in 2005 and eventually into digital twins in 2011. In 2012, the concept of digital twin was revisited by the National Aeronautics and Space Administration (NASA). They characterized the digital twin as a multiphysics, multi-scale, probabilistic, ultra-fidelity simulation that replicates the condition of a corresponding twin based on the historical data, real-time sensor data, and physical model. In 2016, Grieves defined the digital twin as a set of virtual information constructs that fully describes a potential or actual physical manufactured product from the micro atomic level to macro geometrical level. At its optimum, any information that could be obtained from inspecting a physical manufactured product can be obtained from its digital twin [33].

In the recent years, the term digital twin gained prominence, and the Internet of Things and the digital transformation in general makes this concept interesting and accessible to a wide variety of sectors and applications. A digital twin is usually a description of a process or a system that has been supplemented with real-time. The description itself might range from a simple system schematic to a dynamic numerical simulation model, but it becomes a digital twin the instant it is linked to real-world data.

2.4.1 Definition, Background and Evolution of DT

According to Wikipedia, a digital twin is a live digital coupling of the state of a physical asset or process to a virtual representation with a functioning output. In terms of manufacturing, the concept can be explain in different ways, whilst in a simple words, it is a digital replica or representation of a physical object or an intangible system that can be studied, edited and tested without interacting with it in the real world, hence avoiding negative consequences. The fundamental premise is that a real thing or asset has a digital counterpart in the virtual world. DT can be useful for researching control systems for generating and regulating supervisory step-points in order to improve power plant performance. It is also contributes to another effort to increase the flexible power plant operations [34].

As mentioned in the earlier paragraph, digital twin is a method of creating a physical prototype and a virtual simulation from that prototype to be connected in real-time. From the researchers' and engineers' point view, digital twin is a simulation technology that acts as a bridge between a physical and digital world, offering industrial firms new options to carry out smart production and precision management. Digital twin is a virtual copy of the system containing all the components connecting to the same logic controller in real-time. Some physical devices require interconnection in order to optimize intelligent systems. In turn this, the basic concept of digital twin is a simulation method that incorporates several disciplines, multiple physical quantities and numerous scales. It works with today's most popular smart sensors, 5G connectivity, cloud platforms, big data analysis, artificial intelligence and other technologies. Based on massive data resources, a virtual model in digital space is constructed, the mapping link between digital virtual body and physical entity is established, and a "mirror" of entity is formed [35]. In reality, digital twins are digital Clones created from a device or system. This Clone is also known as called digital twin. It is a virtual and dynamic simulation of solid things built on an information platform. Ideally, the digital twin can provide all information measured from the actual product.

The digital twin is an intermediary step between the digital world and the physical worlds that is rapidly progressing beyond information modeling and enabling asset-centric organizations to converge their engineering, operational, and information technologies for immersive visualization and analytic visibility [35]. A digital twin, in most cases, may be continually updated from numerous sources, such as sensors and continuous surveys, to represent its near real-time status, operating condition, or position. The goal of a digital twin is to recreate the power system in real-time. The simulations generated will aid in the development and planning of future prospects and upgrades within the process or product. This technology reduces production costs by eliminating the need for costly

physical testing or modifications to items or processes. The prospects of this technology also bring more confidence to increase production performance and help complicated decisions, minimizing costly downtime to robotics or machines [34].

2.4.2 Challenges and Motivation of Digital Twin in Power System Network

The power system network is a highly complicated man-made system. The utilities spend a significant amount of time and energy to manually maintaining, updating and exchanging information between various systems.. Inconsistencies in data communication, as well as a lack of data interchange, can have drastic implications, such as increased expenses, redundant work, poor system performance, and even system-wide outages [36]. Whilst the capabilities of the digital twin technique pair with improved resolution, data sources are theoretically bigger for analysing the regulation of power system stability. Scenario planning and decision optimisation utilizing a live data model provide operators with a unique chance to improve network dependability and customer experience. DT technology can be used to intelligently control power plants. The virtual power plants are built by creating high-fidelity simulation models of many subsystems of actual power plants. Real-time monitoring, fault diagnosis, and accurate operation of the power plant equipment may be accomplished through the operation and administration of the virtual power plant, assuring the safe and stable operation of the power plant.

To realize the true potential of digital twin idea, a comprehensive strategy to DT data storage, administration, analysis, and validation is required. Because modeling dynamic power system phenomena is fairly complicated, determining the detail-level of the power system model might be a significant issue for digital twin implementation. While an overly simplified model may not reveal the value that a digital twin promises, taking into account plenty of electrical equipment data, measurement devices, and a massive amount of signals to enrich the digital representation of the power system.

Chapter 3

Load Modelling

3.1 Introduction

Load modelling has long been recognised as one of the most critical aspect of power system modelling. The majority of the existing load models were built many years ago, after considerable changes in load structure and characteristics over time. Load modeling is the representation and application of electrical equipment for power system studies, either individual or as a group [2] [37]. Considering loads have a substantial influence on the system, power system planners and operators attempt to precisely estimate loads in order to examine system stability. However, accurately describing loads in a mathematical model is quite challenging. For load modeling, there are two primary approaches: component-based modeling and measurement-base modeling. The former is based on bus load components, whereas the latter is based on power system measurements. In load modeling, there are two important factors. The first factor is the determination of the mathematical model that represents the load characteristics. The second factor is the estimation of the parameters of the determined mathematical model. The composite load model is addressed in this chapter and also the accuracy of dynamic load model. It has both static and dynamic load characteristics. The ZIP model and the induction motor model are used for the static and dynamic load models, respectively.

3.2 Importance of Load Modelling

Due to the blackout power system in many countries, operators began to pay more attention to load modelling. Inappropriate representation of system loads has usually lead to the discrepancies between the recorded and simulated system responses. There is a renewed interest in both industry and academic for load modelling, due to appearance of new types of loads and modern nonlinear electrical and electronic equipment offering increased efficiency and controllabillity, such as LED light sources, adjustable speed drives, inverter-interfaced distributed generation, and also plug-in-electric vehicle chargers. Planners and operators of power systems require results from stability studies in order to make appropriate decisions in the short and long term basis [38]. These studies are required to evaluate the performance and limitations of the power system components when subjected to several operating conditions that may compromise the stability of the system. Their results often verify the level of financial investment, capital expenditures and other economic costs. Selections are performed to ensure continuous operation of the power system. Therefore, adequate, modelling of all component is more complex to compute a correct and realistic results. Among all components of the electrical power system, load characteristics should be accurately modeled as a result of their significant impact on the dynamic behavior of the power system. Historical incidences of inadequate load modelling could disastrous consequences, including Sweden blackout [39] and the collapse of Tokyo network [40] which occurred in 1983 and 1987, respectively.

Due to the aforementioned consequences, from the operators' perspective, they try to accurately model loads in order to analyse their system stability. Considering that loads have significant impact on the system and have a variety of components. In addition, it is very difficult to exactly describe loads in mathematical method. It is presented as a composite load model or an aggregated load model. They can be calculated by estimating the parameters of the specified model and replacing large portions of the distribution system, in the dynamic equivalent. As a result, the computational efforts would be also significantly reduced.

3.3 Implementation of Load Models

The existing load models can be divided into two groups, there are the static load models and dynamic load models. The static and dynamic load models are classified according to the effect of the voltage on the load. If the load variation depends only on the instantaneous voltage input and is unrelated to the preceding voltage inputs, the static load model is used. However, if the load characteristics are affected by all of the voltage inputs over time, the dynamic load model needs to be used. For example, an electric lamp represents a static load, whereas an induction motor represents dynamic load. The word 'static' and 'dynamic' refers to the type of studies these models are suitable for. The static studies are about the steady state analysis of the system, hence static load models would suffice, while the dynamic studies are about the transient analysis of the system, where modelling of loads using differential equations is required to capture variation of the response with time.

3.3.1 Static Load Model

Static load model is one of the two main category of load models. It is mostly used for representing general residential loads that do not consist of large induction motors and drives. the static load model is used when the load variation is only dependent on the current voltage input and is unrelated to the preceding voltage input. The static load models for active and reactive power are stated in [1, 2, 37, 41, 42], as a function of the bus voltage and frequency at any instant. In this paper we are only consider voltage dependence.

3.3.1.1 Exponential Static Load Model

The static exponential load model is one of the most frequently used load models around the world. It is described by Equation 3.1.

$$\begin{aligned} P &= P_0 \left(\frac{V}{V_0}\right)^{n_p} \\ Q &= Q_0 \left(\frac{V}{V_0}\right)^{n_q} \end{aligned} \tag{3.1}$$

Where P and Q are active and reactive power of the load at voltage V. P_0, and Q_0 are normally taken as the values at the initial operating conditions. The parameters of this model are the exponents n_p and n_q, with these exponents equal to 0, 1 and 2, the load can be represented by constant power,constant current and constant impedance, respectively. For composite loads, their values depend on the aggregated characteristics of the load components. Static load models are often sufficient to represent the system response some seconds after a disturbance, but for longer time scale phenomena such as voltage recovery, models that reflect these dynamics may be required.

3.3.1.2 Polynomial Static Load Model

In addition to static exponential load model, another frequently used static load model is polynomial load model. It can be implemented in different forms, either with frequency dependence considered or not. In this thesis, frequency dependence is neglected, and the voltage dependent form of the polynomial load model is as follows in Equation 3.2

$$\begin{aligned} P &= P_0 \left[a_1 \left(\frac{V}{V_0}\right)^2 + a_2 \left(\frac{V}{V_0}\right) + a_3\right] \\ Q &= Q_0 \left[a_4 \left(\frac{V}{V_0}\right)^2 + a_5 \left(\frac{V}{V_0}\right) + a_6\right] \end{aligned} \tag{3.2}$$

This load model is also referred to as the ZIP load model, which is consisting of the sum of the constant impedance (Z), constant current (I) and constant power (P) terms. Where V_0, P_0 and Q_0 are normally taken as the value at the initial operating conditions. The parameters of this polynomial model are the coefficients (a_1 to a_6) and the power factor of the load. In this thesis we consider that the active power are voltage dependent so that we neglected the reactive power terms from the ZIP model. As a result the equation becomes Equation 3.3.

$$P = P_0 \left[a_1 \left(\frac{V}{V_0} \right)^2 + a_2 \left(\frac{V}{V_0} \right) + 1 \right] \tag{3.3}$$

When the traditional static load models are not sufficient to represent the behavior of the load, the alternative dynamic load models are necessary.

3.3.2 Dynamic Load Models

In many research dynamic load model defined as a model that expresses the active and reactive powers at any instant of time as functions of bus voltage magnitude and frequency at a past instant of time and, usually, including the present instant. Dynamic loads are loads whose responses are dependent on the states in which the system and load previously were in time. Their models are usually expressed in different equation forms relating the real and reactive power with voltage and frequency. Here, also frequency dependence is neglected. They are often used to represent loads that have substantial amount of induction motors and electric drives. The general mathematical formula of dynamic load model are almost similar to those of static load model. The difference is based on the addition of time dependency factor.

3.3.2.1 Exponential Dynamic Load Model

Authors Karlsson and Hill of [1] have proposed a load model with exponential recovery, due to the large amount of electric heating loads in Sweden and its effect on voltage stability. Equation 3.4 and 3.5 are for a widely used exponential load model, which is based on generic forms representing the responses observed by induction motors, heating loads and tap-changers after a voltage change[43]. The exponential recovery load model aims to capture the load restoration characteristics with an exponential recovery process expressed as an input-output relationship between powers and voltage, where the real power consumed by the load are assumed to be related to the voltage in the following nonlinear manner [44] and [45].

$$P_s(v) = P_0 \left(\frac{V}{V_0}\right)^{n_{ps}} \tag{3.4}$$

$$P_t(v) = P_0 \left(\frac{V}{V_0}\right)^{n_{pt}} \tag{3.5}$$

$$T_p \left(\frac{dP_r}{dt}\right) + P_r = P_s(v) - P_t(v) \tag{3.6}$$

$$P_l = P_r + P_0 \left(\frac{V}{V_0}\right)^{n_{pt}} \tag{3.7}$$

3.3.2.2 Dynamic Load Model of Induction Motor

Among the dynamic load of a power system, induction motors constitute the major portion, and it is generally accepted that, for transient voltage stability, their effect prevails [1]. The induction motor (IM) is the most widely used and customary type of electric machine in home, business and industry. According to statistically, about (50-70)% of all electrical demand is consumed by electric motors with about (90)% of this being used by induction motors. Such motors dominate industrial loads to a far greater degree than they do commercial or residential loads [2]. The single-phase induction machine is utilized for the majority of domestic uses, whereas three-phase induction machines are needed for higher power industrial applications including electric ships, pumps, and compressors. In this model, the active and reactive power is represented as a function of the past and present voltage magnitude of the load bus. Commonly derived from the equivalent circuit of an induction motor, shown in Figure 3.1.

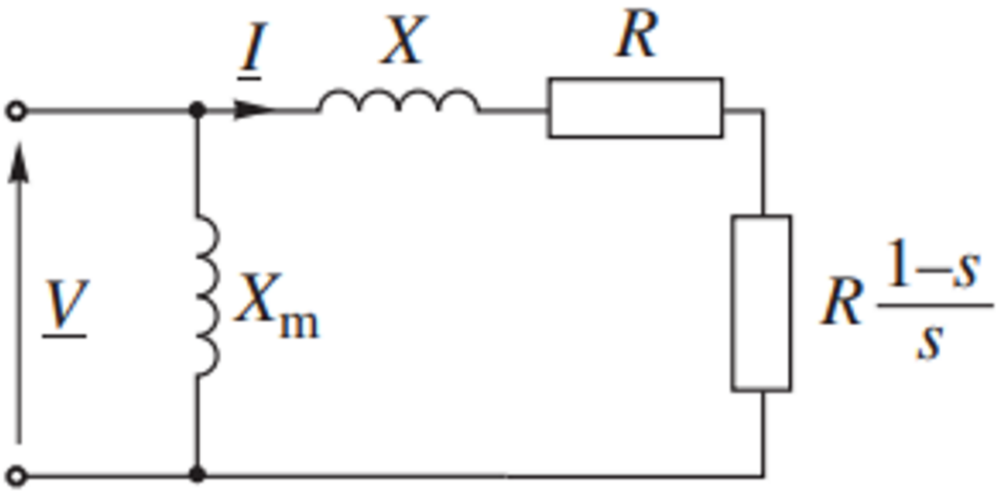

FIGURE 3.1: Simplified equivalent circuit of induction motor

Where R_s and R_r are static and rotor resistances, respectively, X_s, X_r and X_m are the static, rotor and magnetizing reactance, respectively, and s is the rotor slip defined as $s = \frac{(\omega_s - \omega)}{\omega_s}$. The induction motor model is considered as a physical-based model.

3.4 Load Model Parameter Identification

For load modeling, two approaches have been used. First, a field test-based approach, also known as a measurement-based approach, obtains the load model by measuring the system's response without the need for prior knowledge of the load's physical characteristics. It uses sensors like smart metering or phasor measurement units (PMUs). The second approach is component-based , in which the load model is obtained by aggregating the models of individual components. In general, both approaches can be used when a load models has several components, such as the ZIP load model and induction motor load model executing together. If the load only consists of one component, the measurement-based approach is normally used [46].

3.4.1 Measurement-Based Approaches

The measurement based approach is a top-down method or behavior-based approach. In this methodology the system events at substations or feeders of interest are recorded to obtain data representing the characteristics of the connected load. These events could be small or large disturbances such as switching or lightning events that changes the system bus voltage and frequency. The recorded power system events and disturbances are used to drive the required load models. In order to develop load models and estimate credible parameters, it is necessary to postulate the initial load model structure in advance. The load response indicates that active and reactive power fluctuations are monitored by measuring devices when the disturbance occurs. The data collecting tools implemented in the real power grid, such as phasor measurement units (PMU), current voltage transformers, smart-metering and power quality meters [46].

The key advantages of this approach are the use of dynamic response data of the load from actual grid system and the simplicity of applying it to any kind of load. However, the drawback of this approach is the lack of large disturbance measurement data needed for appropriate parameter estimation due to the robustness of the system [7]. The measurement-based methods use voltage and active power measurements data from the smart meters or phasor measurement units. The following subsections provide a description of certain measuring equipment.

3.4.1.1 Phasor Measurement Units

A Phasor Measurement Unit (PMU)is a device that collects data from a specific location on the electric grid in order to measure the phasor, magnitude and phase angle of voltage and current. The measurement is coordinated with a shared time source. Synchrophasor refers to the estimated phasor that has been time-synchronized. It was calculated by applying the Fourier Transform to the alternating signal. When timestamped, a phasor turns into a synchrophasor. Therefore, a precise time source is required e.g. a Global Positioning System (GPS) or Precision Time Protocol (PTP). PMU reporting rate are normally below 60 frames per second [47], although they can be higher. The sampled measurement values are digitized and packet into frames for transmission and streamed to a substation or control center phasor data concentrator (PDC – sometimes also called synchrophasor vector processor [48]).

PMU sensor networks improve the power system's observability, allowing for the monitoring of transient and dynamic events. A PDC does the necessary data processing, essential aggregating and time-aligning the samples for subsequent analysis. These readings are shown by the PDP module in the control room, which also allows the operator to see power fluctuations as well as frequency and angle deviations. Many sophisticated applications, such as dynamic security improvement and online monitoring of system dynamics, are achieved in control center by phasor data processing.

Tens of thousands of PMUs have recently been installed in transmission networks all around the world. PMU offers the chance to switch out the conventional manual adjustments required by SCADA systems with a system that makes decisions and transmits control signals by itself.

3.4.1.2 Smart-Metering

In article [49] highlighted that smart metering has been recognized as a major part of the smart grid system. It has been regarded as a tremendous, hopeful possibility that would allow residential electric customers to reduce their usage and lower their prices. In actually, a smart metering system is composed of smart meters, control devices and a communication link. The main goal of the smart metering system is to lower greenhouse gas emissions while also lowering monthly fees for consumers. The key element of this system is the smart meter which is the combination of all energy metering and intelligence. Ordinary electromechanical meters and smart meters are fundamentally different from one another. However, there are a number of issues with the electromechanical meters that we use today, such as their lack of configurability and poor accuracy. With varied working temperatures and conditions, they have several moving parts that are prone to wear down over time. They just offer statistics on how much energy is being measured, and these data are useless for encouraging energy efficiency. in order to improve energy efficiency, demand control, and energy saving, smart meters were implemented. Smart meters have the ability to communicate with one another and carry out local and distant command signals. they provide practical methods for resolving issues with the outdated grid.

3.4.2 Component-Based Approaches

This approach, also known as the the bottom-up approach or knowledge-based approach, depends on the understanding of individual load components to construct an aggregate load model. The component based method is illustrated in Figure 3.2 with a typical load model structure and an exemplary set of parameter values. According to this figure, the load may be decomposed into several sectors such as residential, industrial, commercial, and agricultural depending on load consumption. In order to accurately represent their mix within the overall load demand, they are further separated by types such as resistive, inductive, power electronics, etc.

The main advantage of this approach is its independence on the field measurements of the power system and may be used to establish composite load models. Nevertheless, its main drawback is that it does not account for changes in load structure or composition over time caused by seasonal, behavioral or weather related fluctuations. Moreover, determining the composition of load is quite challenging anymore.

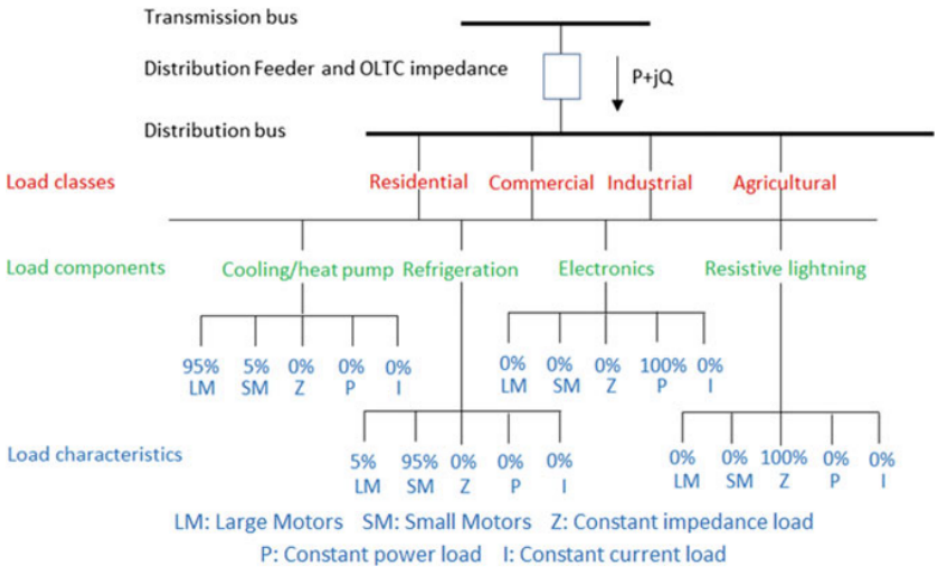

FIGURE 3.2: Component based load modelling approach example

3.5 Composite Load Model

The composite load models are intended to take into account the effects of various components. It is a combination of a static load, a generic dynamic recovery load and an aggregate induction motor load. An adequate load model should incorporate both static and induction motor components. Many research have been conducted on the composite load model, which comprises of both static and dynamic load characteristics. There are several variants to composite load models due to the choice of their exact composition [50][51]. All the static load components are accounted for by the static load and expressed by d and q current components of resistive and capacitive loads, or by a ZIP model as implemented in [37]. To represent the dynamic attributes of load, most composite load models use the equations of a third order IM model due to their predominance. Figure 3.3 shows the equivalent circuit of the ZIP model with separated constant impedance, current and power components in parallel with a basic illustration of an induction motor model. The ZIP part representing the static loads can be described

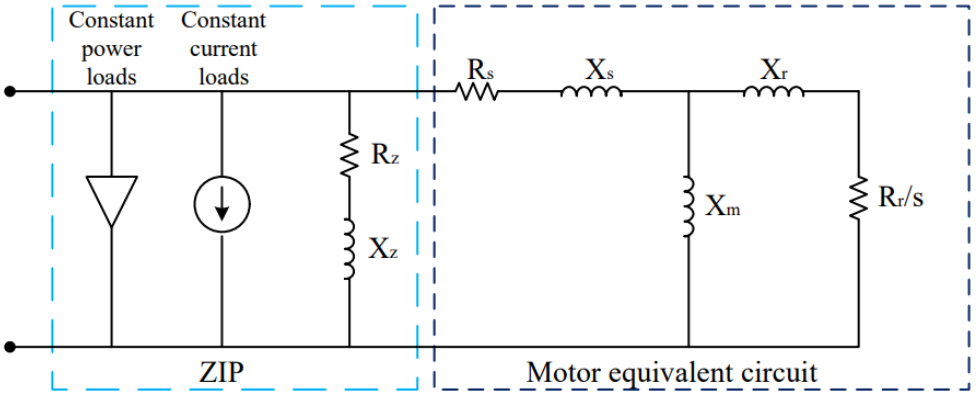

FIGURE 3.3: Composite load model

similarly as equation 3.1 and 3.2.

A new power system load model is proposed [2] which will be an improvement in the accuracy of the static and detailed dynamic load models. This new load model must fulfill the following requirement

1. The model must be as simple as possible
2. Model must accurately represent the dynamics of composite power system load
3. Model must adapt easily to existing stability programs
4. Model must have parameters which are identical from actual power system load measurement

Furthermore, in our load modeling experience, we have discovered that, in addition to these above objectives, there are more particular issues that must be addressed. The first one is the intended applications of the load model. The load model we built is mainly for power system stability simulation and control, whereas this thesis focuses only on voltage stability and should easily compile in DynPSSimPy program tool. The second concern is the application range in which the model is applicable. In fact, there is no universal load model that can be applied to all cases. Since the load consists of various components with different characteristics. For instance, under worse cases, such as those near the voltage collapse point or dramatic voltage dips lasting for several seconds, some load components may show highly nonlinear characteristics, and some motors will drip off. We wish to design a general load model based on the aforementioned load model aspects that should be valid in most cases in power system stability analysis. In this thesis, we developed an aggregate dynamic load model.

3.5.1 Accuracy of Dynamic Load Model

In this thesis we have developed a dynamic load model that describes real power responses to voltage step. This model was selected because it is suitable as demonstrated by a large number of trials at different substations for modeling any type load with a considerable component of load devices. The model is presented here for completeness of discussion. First order differential equations, which are described in Equation 3.10, are used to develop the mathematical formula that defines the interplay between voltage and load power.

In voltage stability studies [52], the dependence of both active and reactive power on frequency is generally assumed negligible because of the limited variation of the latter; by representing their rated levels by a zero subscript, only considering on the active power absorbed at the bus of interest can be then expressed as follows

$$P_s(v) = P_0 \left(\frac{V}{V_0}\right)^{n_{ps}} \tag{3.8}$$

$$P_t(v) = P_0 \left(\frac{V}{V_0}\right)^{n_{pt}} \tag{3.9}$$

$$P_d = x_p + P_t(v) \tag{3.10}$$

$$T_p \dot{x_p} = P_s(v) - P_d \tag{3.11}$$

Furthermore, a load model is proposed in state space form to provide parameters which can easily be determined by an identification process and to facilitate incorporation

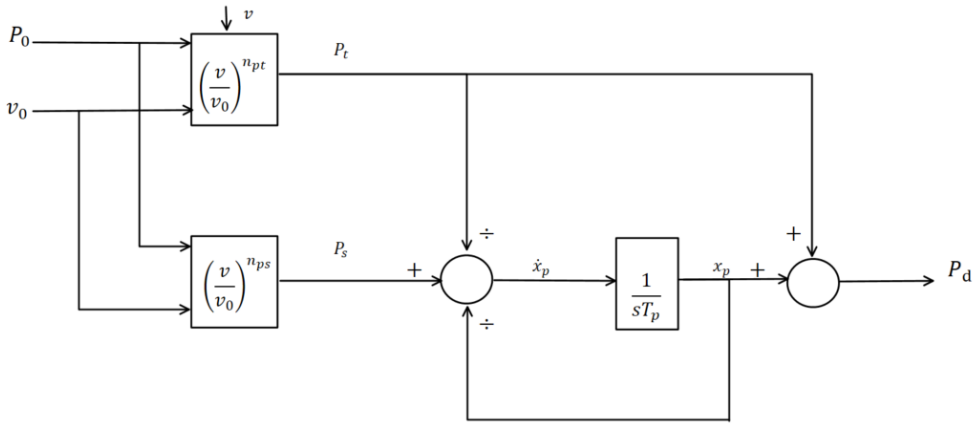

FIGURE 3.4: Dynamic load model

of the equations into the stability program solution. The most frequently used is the exponential composite load model, which is aggregate loads consisting of a static load model in parallel with the equivalent dynamic load model. The model is developed as a non-linear first-order equation to represent the load response as shown in Figure 3.4.

Chapter 4

Simulation Results

In this study, time domain simulation is applied to study the dynamics of voltage stability. The system used for carrying out the dynamic simulation is the Nordic 44 Test system. Figure 4.2 shows a one-line diagram of the test system. The programming was also tested on a simple network, the Kundur Two Area system. The dynamic load model is implemented in Hasle station or on Bus 9, shown in Figure 3.4. It is also described in Chapter 3 as a function of voltage dependence only. Voltage stability studies are one of the major concerns in power system operation, where the ability of a power system to maintain an acceptable voltage at all nodes in the system under normal conditions and after being subjected to disturbances is analyzed. There are three case studies in this thesis regarding the variation of the dynamic load response with dependence on the three parameters. The parameters are n_ps for steady state load exponent, n_pt for transient load exponent, and T_p for load recovery time constant.

The power system network model and the dynamic information are integrated into the simulation software DynPSSimPy, Dynamic Power System Simulation Python, which is used as a simulating environment in this thesis. In our case, the Nordic 44 Test or Kundur Two Area test systems are first solved in steady-state to observe their stability. This system will be a revised system with a new composite load connected at Bus 5101 or at Bus 9 with load composition and dynamic parameters at every run, respectively, in the Nordic 44 Test and Kundur Two Area Test. Initially, the power system network is brought to a steady-state condition in order to test the voltage variation following a fault or disturbance in the system.

In this thesis, simulation time series from the Nordic 44 Test or Kundur Two Area are used to test the dynamic load model. Our presumption is that utilities and system operators routinely assess N-1 contingencies. The system is already safeguarded from these unforeseen events. As a result, we first provide a brief overview of the DynPSSimpy

and networks. Next, three separate simulation tests are run using the Kundur Two Area system 0r Nordic 44, and the results of each test are shown in the subsections that follow.

4.1 Dynamic Power System Simulator in Python

This program, DynPSSimpy, is an alternative to the DigSilent PowerFactor program and this software tool has been developed by Doctoral student Hallvar Haugdal [53]. It is mostly used to simulate electric power transmission network. It offers several valuable features and is mostly used for steady state (load flow) and dynamic studies (fault application). Moreover, it is utilized to develop and implement dynamic models as well as to simulate power systems. Article [54] covers the working principles of the software, which is an open-source package for running dynamic RMS simulations of preferably small to medium-sized power systems. This software have several benefits, including flexibility, transparency, and expandability. As a consequence, the package could arguably benefit researchers and students by providing a foundation for developing an intuitive understanding of power system operation and control due to the requirement of creating self-made models that require real-time interaction and a fundamental understanding of their operation. Furthermore, the package is entirely built within a Python environment, promoting the use of built-in Python packages and libraries, which proves to be tedious and complicated to interact with for other available software [54]. The package relies on the Differential-Algebraic Equations (DEAs) describing the dynamics of the system. The set of dynamic equations from generating units and dynamic loads be represented by Equation 4.1 and the set of network equations be represented by Equation 4.2

$$\dot{x} = f(x, y) \tag{4.1}$$

$$0 = g(x, y) \tag{4.2}$$

It is further based on solving linear equations on the form $YV = I_{inj}$, where Y is the system admittance matrix, V is bus voltage and I_{inj} is the injected bus current. Therefore, current injection models are favoured because of their easy of interaction with the rest of the system. The dynamic simulations, on the other hand, rely on solving Ordinary Differential Equations (ODEs) and allowing the use of any suitable integration method, allowing the user to describe on the trade-off between computational burden and solving accuracy by selecting appropriate solvers in the Python environment. This thesis is utilizing an new version of the package 2021, the dynamic load models are presented by class shown in Figureure 4.1. It substantially simplifies the implementation of new models and provides a more visible and understandable framework. The model given by 3.4 has been validated for all the cases presented.

```python
class DLOAD:
    def __init__(self):
        self.state_list = ['x_p']
        self.int_par_list = ['f']
        self.input_list = ['v','v_0','P_0']
        self.output_list = ['P_d']

    @staticmethod
    def initialize(x_0, input, output, p, int_par):
        x_0['x_p'] = output['P_d']
        input['v_0'] = 1.0


    @staticmethod
    def _update(dx, x, input, output, p, int_par):

        P_s = input['P_0'] * (input['v'] / input['v_0']) ** p['nps']
        P_t = input['P_0'] * (input['v'] / input['v_0']) ** p['npt']

        P_d = x['x_p'] + P_t

        dx['x_p'] = 1/p['T_p']*( P_s -P_d)
        output['P_d'][:] = P_d
```

FIGURE 4.1: Class of Dynamic Load Model in Python

4.2 Network Description

In this section, two networks are presented and tested in the case studies. The first network is a simple network, which is known as Kundur Two Area System. This network has only two area modes. The second network is complex and realistic network, which is known as Nordic 44 Test system. The network model comprises information on buses (total numbers and types), line and shunt impedances, the power generated and load demands. Dynamic information includes transient characteristics of generators, exciters, governors, and loads. The dynamic simulation is valid in both networks for testing the system stability. Therefore, in this thesis we prefer to use a simple network system to verify the dynamic load model. The following subsections are presented in the description of both networks.

4.2.1 Nordic 44 Test System

Nordic 44 Test is an aggregate dynamic power system simulation model designed for analysis of dynamic phenomena in the Nordic power grid. This network was initially developed at the Norwegian University of Science and Technology (NTNU) and had gone through many iterations before reaching its current version [55], and the system parameters used for this thesis can be found in Appendix [A]. The Nordic 44 Test is among the largest and most complicated systems, including Norway, Sweden and Finland as shown in Figure 4.2. It is divided into distinct areas, ie. in Norway there are eight areas [NO1, NO2, NO3, NO4, NO5, NO6, NO7 and NO8], Sweden is divided in four areas [SE1, SE2, SE3 and SE4] and only two areas in Finland [FI1 and FI2]. The total number of buses in this network is 44, implying that the name of the network is derived from those buses. There are a total of 12 transformers in the network, with nine of them in Norway, and the rest in Sweden. It consists of 61 generators with various control systems such as exciter, turbine, governor and stabilizer. However, not all generators are installed with governors and AVRs, and for those with these control systems, they will be the same for all generators. It also comprises 67 transmission lines with 420 kV and 300 kV, as well as 43 loads in various nodes. Furthermore, this test network is used to evaluate the performance of the different implemented units in a large and more complicated system than the estimate and straightforward Kundur Two Area system. It is presumed that the dynamic load model is connected at Hasle station in this test network.

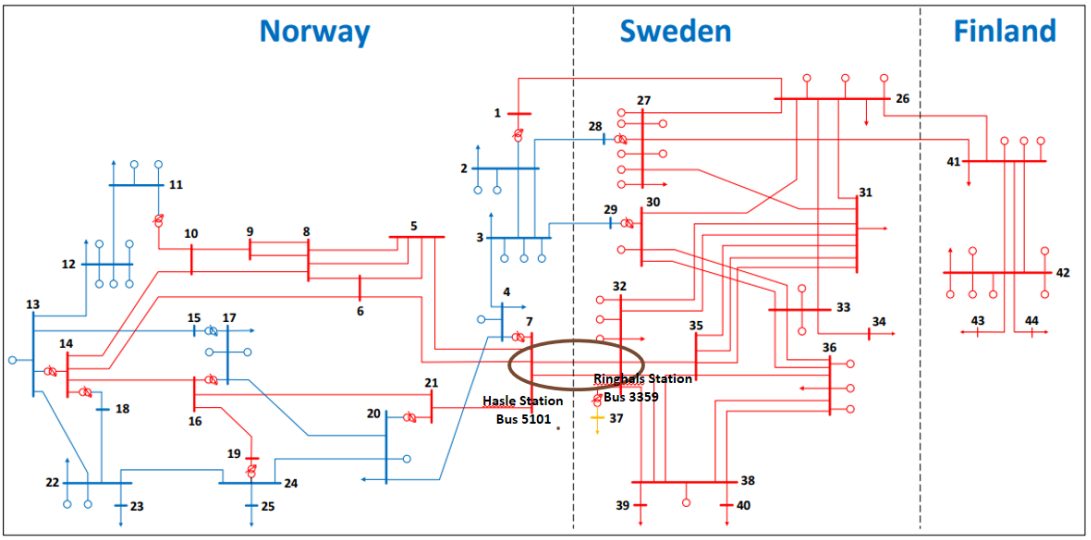

FIGURE 4.2: Nordic 44 Test System one-line diagram

4.2.2 Kundur Two Area System

Kundur Two Area Test system is a simple and an estimate power system model that is used for a wide range of research related to operation and control. It was originally developed by Kundur in 1991 for simulating the interactions between different areas connected by weak grids [56]. It consists of 11 buses, 4 generators with different control systems exciter, turbine, governor and stabilizer, and 8 transmission lines with 230 kV and 20 kV, and only two loads in Bus 7 and Bus 9. The overall parameters of this network are list in Appendix [B]. Furthermore, a slightly modified of the system is shown in Figure 4.3. Dynamic load model represent any load component having a controllable power injection to the network. For this thesis, Kundur Two Area will mostly be used for testing purposes and for verifying the implemented models as expected in the simulation results.

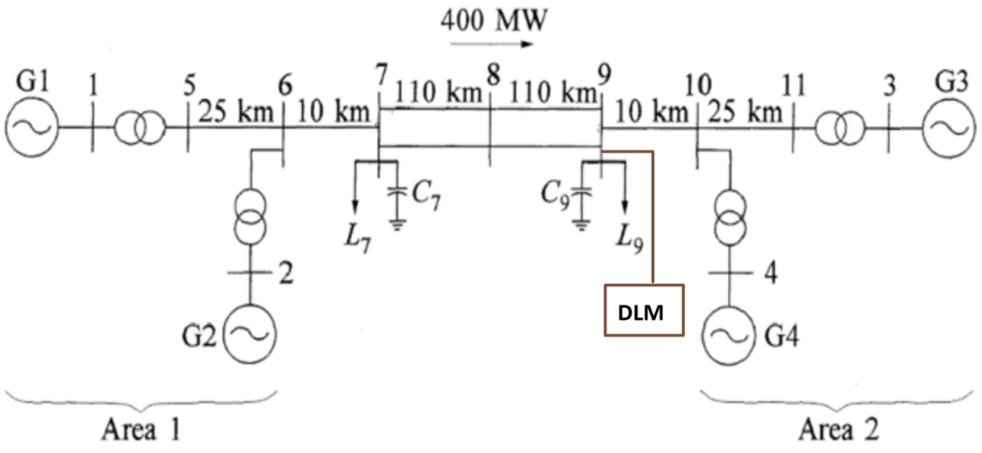

FIGURE 4.3: A single line diagram of Kundurs Two-Area System

4.3 Case Study

In this simulation study, three different case studies are tested. The first case test is a single line trip on the system, with different parameters of the dynamic load model. In this case study the system will be verified as a dynamic load model. The second case study is the impact of the load model on the voltage stability. By applying multiple transmission lines trips with different values of recovery time constants and a comparison of the results at different values of the steady-state load exponent, ie. $n_{ps} = 0$ and $n_{ps} = 2$. The third case study is on the impact of the load models on the power oscillation. On the third case, a short circuit event is applied. The dynamic load model, which is briefly described in Chapter 4, is connected in Hasle station or Bus 9 at zero second, respectively, in Nordic 44 Test or Kundur Two Area Test. Their initial parameter of power input and nominal bus voltage of the dynamic load model in Kundur Two Area are constant and their values are 0.058 p.u. and 1 p.u., respectively.

4.3.1 Case 1: To Verify the Load Models

In this case we used a Kundur Two Area network, to verify the dynamic load model response when an incidence occurred in the system. The load model is known as dynamic load model, only if the steady-state and transient load exponents are not equal. Thus, we test this combination of load exponents, and consider the steady-state load exponent equal to zero, ie. the value of $n_{ps} = 0$, whereas the transient state load exponent was equal to two, i.e $n_{pt} = 2$, while the recovery time constant would be varied [0.1, 1 10], as the parameters are shown in Table 4.1. In Kundur network, the dynamic load model was connected in Bus 9 and their initial input power was set $P_0 = 0.0586$. For a particular operating point in Kundur network, additional load in a specific pattern increases, which causes a voltage collapse. It is called the load margin. For this network the load margin was $58.6MW$. This indicates that the power generated must be equal to the demand plus the line losses. In the power system network there are many factors that the system would oscillate and voltage-step is achieved due to sudden load change, short circuit and line outages.

In this case, L-7-8-1, one of the double transmission lines between Bus 7 and Bus 8, was tripped, at 1 second. The objective of this case study , as stated in the preceding paragraph, is to validate the dynamic load response caused by step-voltage in the system with different recovery time constant. As is common knowledge, the system's bus voltage is lowest in the area that is overloaded. The weakest bus voltage in the Kundur Two Area system was on Bus 8. This is due to the long transmission line. It can be seen from a single line diagram Kundur network that the power flowing between these lines

are equal to 400MW. A line outage of one of these tie lines is presumed to impact the dynamic load model response, however, the system stability was not significantly influenced.

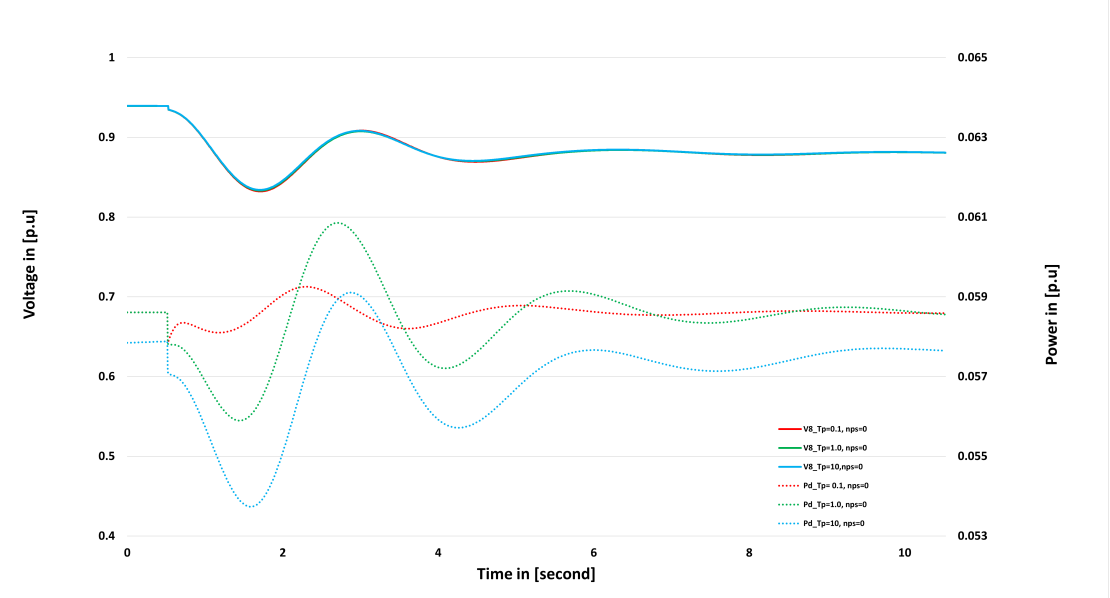

FIGURE 4.4: Case 1: One line was tripped in Kundur Two Area System, L-7-8-1. Voltage drop at Bus 8. When the steady-state load exponent is equals to zero, transient load exponent equal to two and recovery time constant are varied. Dynamic load model respond were varied due to the recovery time constant. Left and right vertical axis refers to voltage magnitude and desired power response, respectively.

TABLE 4.1: Parameters of the dynamic load models with different recovery time constant

V0	P0	ntp	nps	Tp
1	0	2	0	0.1
1	0	2	0	1.0
1	0	2	0	10

TABLE 4.2: Parameters of the constant resistive load models with different recovery time constant.

V0	P0	ntp	nps	Tp
1	0	2	2	0.1
1	0	2	2	1.0
1	0	2	2	10

The simulation result in Figure 4.4 presents the dynamic load model response to the step-voltage due to the one line outage in the system. The voltage magnitude at Bus 8 was step reduction, after a single line was tripped. Figure 4.4 presents the voltage magnitude and dynamic load model response in one Figure with two scales, left and right vertical axis, respectively. The solid lines refer to the voltage magnitude and the dotted lines refer to desired power. The voltage magnitude at Bus 8 has dropped from 0.925 p.u. to 0.785 p.u., by 15.13% when the steady-state load exponent equals to zero and the transient load exponent equals two. However, the recovery time constant varies in this case test, the voltage magnitudes at the weakest node are approximately equal. These overlapping curves of different values of recovery time constant [0.1, 1.0 10] are highlighted in solid red, green and blue colors, respectively. On the other hand, when the steady-state load exponent is equal to two, the voltage magnitude at the weakest bus in the system is reduced by 11.89% in all recovery time constant parameters T_p. This is reflecting that the voltage magnitude was not influenced by the recovery time constant when both the steady-state load exponent and transient load exponent were resistive loads, ie. $nps = 2$ and $npt = 2$, as shown in Table 4.2. Therefore, the CRL model is in quadratic relation with the voltage magnitude. As a result the load response is fluctuated with voltage variation. Furthermore, this model could not be affected by the recovery time constant. Both the step voltage and dynamic load response were presented in Figure 4.4. From this case study, a voltage-step occurred in the overloaded area in the system due to a small disturbance and the dynamic load model response appropriately as a load-voltage dependence. Thus, the power system state returns to identical or close the pre-disturbance operating point.

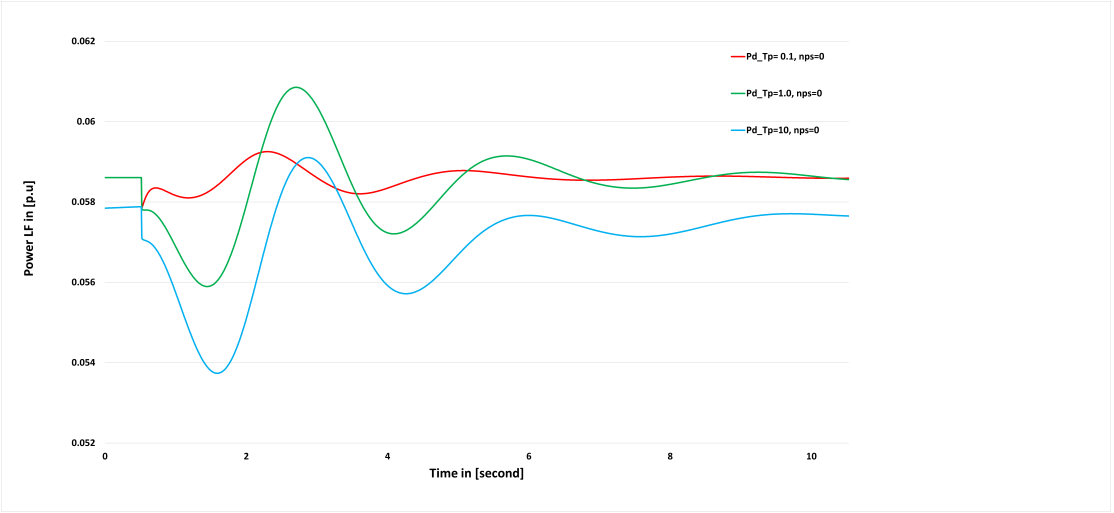

FIGURE 4.5: Case 1 One line was tripped in Kundur Two Area System, L-7-8-1, and dynamic load model response varies according to the recovery time constant

Furthermore, the dynamic load model is used to detect the events and provide a response depending on the recovery time constant as shows in Figure 4.5. When the recovery time constant was extremely small, the dynamic load model was responding rapidly as compared to the longer recovery time constant. From the simulation results, the solid red line has small recovery time constant and desired power responses quickly. It reaches quickly initial power input of the dynamic load model and fast oscillation as compared with the longer recovery time constant. When a longer recovery time constant was applied in the system, dynamic load model response was slower and it took time to reach its initial input power, for example the solid blue line has 10 seconds of recovery time constant. It is observed that the recovery time constant is an important parameter for the dynamic load response. When the steady-state load exponent was set to two, the system was still stable, but the desired output power, P_d did not reach the input power, P_0. This shows that the model refers to a static behaviour.

In general, the network systems have been designed to fulfill the N-1 contingency, reflecting that the system was stabilized after several seconds even if a single line was disconnected. However, the transmission line was overloaded and all the power will flow across the remaining line as shown in Figure 4.7. This indicates that the system has not met the reactive demand, and the short length of the transmission line helps the system in stabilizing. Usually, but not always, voltage collapse involves system conditions with heavily loaded lines. From the previous simulation results, our load models were presented for flexible loads as a dynamic load model. The dynamic load model can be injected or extracted as power into the system. When the system was overloaded in a specific bus, the dynamic load model detects and responds sufficient amount of power into the system.

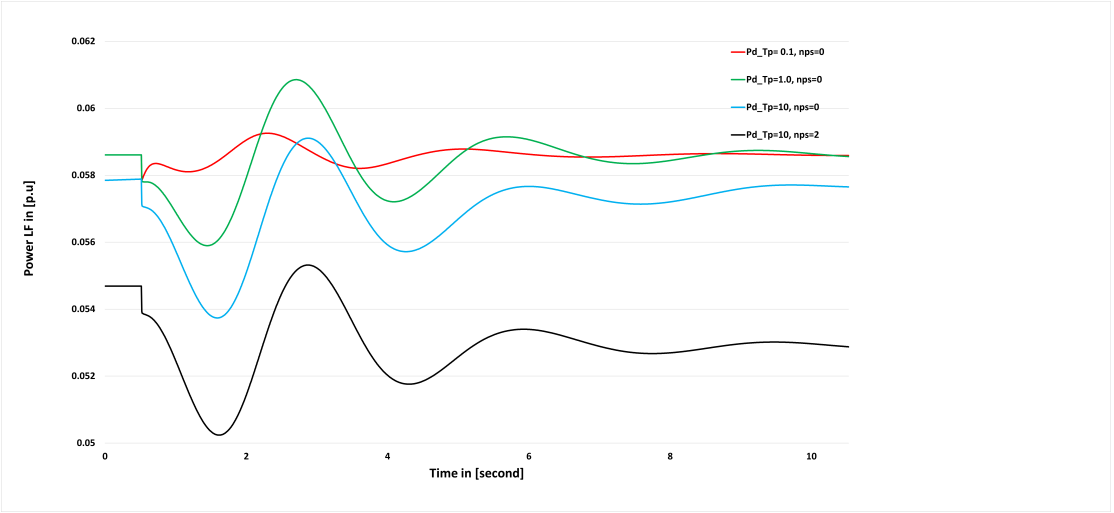

FIGURE 4.6: Case 1 One line was tripped in Kundur Two Area System, L-7-8-1, and dynamic load model response varies according to the recovery time constant and load exponent

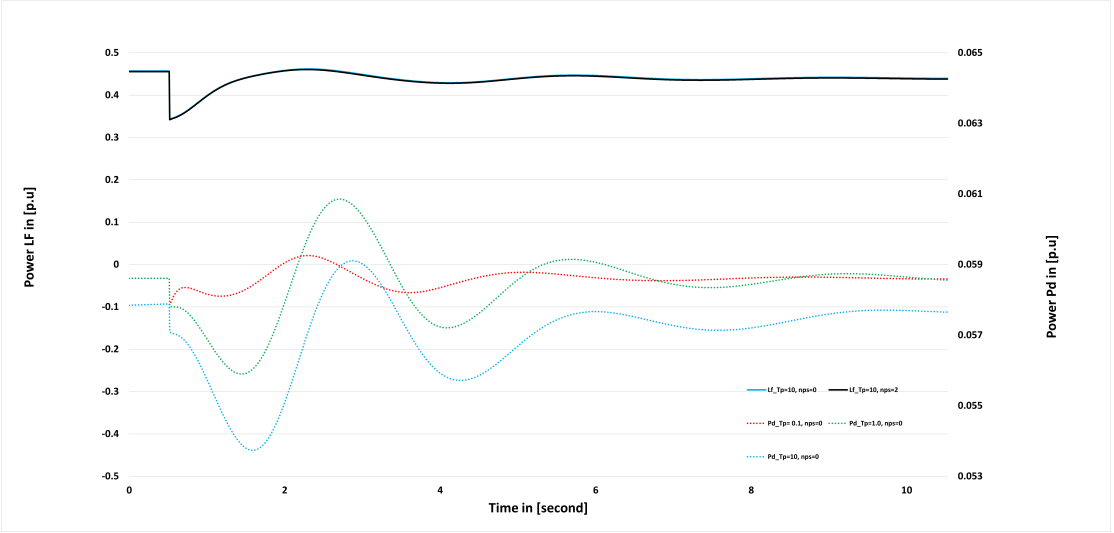

FIGURE 4.7: Case 1 One line was tripped in Kundur Two Area System, L-7-8-1. The load flow of the transmission line, L7-8-2, was overloaded and the desired power output of dynamic load model respond differently according to the recovery time constant, left vertical axis scale refers to load flow, while the right vertical axis refers to desired power output of dynamic load model.

The total power transfer from Area 1 to Area 2 was increased by 0.0586 p.u due to an injection of dynamic load model at Bus 9. This amount of power is transferred through the double transmission lines and share the load flow. When a fault was applied in the system, all power transferred from Area 1 to Area 2 through one line. As a result the remaining line was overloaded. Figure 4.7 presents both the load flow though the remaining line and the desired power output of the dynamic load model. Vertical axes are presented with different scales for load flow and desired power Pd, left and right, respectively.

In the earlier event, the network system was stable after one transmission line was tripped. To verify this, the dynamic load model could also be tested in instability condition. Therefore, in addition to the transmission line being tripped, a sudden load change was applied to the system. Due to those two events, the system might collapse. This depends on the amount of sudden load change in Bus 9. Moreover, it also slightly depends on the recovery time constant as we have shown in Table 4.3. Therefore, sudden load change causes system instability. For instance, additional load was applied in Bus 9, 303 MW and one breaking line was still in the system. This will also lead to voltage collapse, and the node voltage of the system decreases continuously until voltage collapse finally appears. Figure 4.8 shown only the main part of the simulation. Both the desired power output and voltage magnitude at Bus 9 were oscillated and collapsed, right and left vertical axes indicate the scales, respectively. For small recovery time constant, the system was quickly oscillated and voltage collapsed. In order to prevent voltage collapse, the dynamic load model injects positive current into the system and the system will be stable near the operating point. Therefore, dynamic load model can work like a controller by taking action to stabilize the system, by either injection or extraction. In case where the loads are supposed to be reduced based on the measurements in the system, this is simulated by having the dynamic load model inject positive current to the system, which in turn adjusts the net power demand at this bus. For case where an increase in the load demand is needed, injection of negative current to the grid represents increased power demand at the current bus. This action can be performed by moving the control button right or left, as shown in Figure B.1.

TABLE 4.3: Sudden load changes and boundary limits

V_0	P_0	ntp	nps	Tp	Not Oscillated	Oscillated
1	0	2	0	0.1	< 286	$>= 286$
1	0	2	0	1	< 289	$>= 289$
1	0	2	0	10	< 295	$>= 295$
1	0	2	2	0.1	< 303	$>= 303$
1	0	2	2	1	< 303	$>= 303$
1	0	2	2	10	< 303	$>= 303$

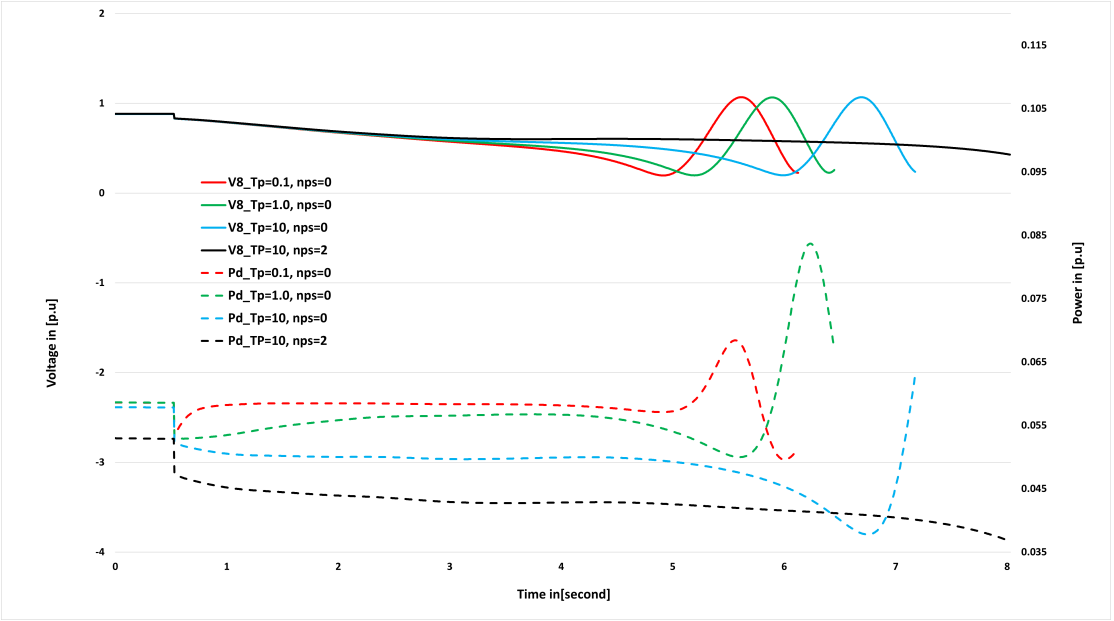

FIGURE 4.8: Case 1 One line was tripped in Kundur Two Area System, L-7-8-1 and sudden load change in the system at Bus 9 with 303 MW. Thus, the system was collapse and the desired power output of dynamic load model respond differently according to the recovery time constant.

4.3.2 Case 2: Impact of Load Models on the Voltage Stability

This case study is intended to demonstrate the impact of dynamic load models on performance of voltage stability. It is based on the load exponents, ie. nps and npt. Parameter values were the same as in the previous case. The dynamic load model was applied at Bus 9 from the beginning of the simulation and the initial power input is set 0.058 p.u.. In this case, line outages cause instability of the system and voltage collapse. The double transmission lines, L-7-8-1 and L-8-9-1 between Bus 7 and Bus 9, were tripped at 1 second and total simulation time was 50 seconds. In all load models the system was unstable and oscillated in different time frames regarding the recovery time constant. However, the simulation results were presented only the main part of the simulation in Figure 4.9, illustrating the tripped lines occurred at 1 second. Special attention should be given to the weakest bus voltage areas in the system. The voltage magnitude at the weakest bus voltage will drop rapidly. It shows that the system was collapsing rapidly when the recovery time constant was extremely small. The solid red line was oscillated rapidly, because its recovery time constant was only 0.1 second, whereas the other simulations were also oscillated later. This delay is depending on the recovery time constant. This is reflecting that the dynamic load model was depending on the recovery time constant. When the recovery time constant has long duration, the voltage at a bus drops slowly and takes time to collapse the system.

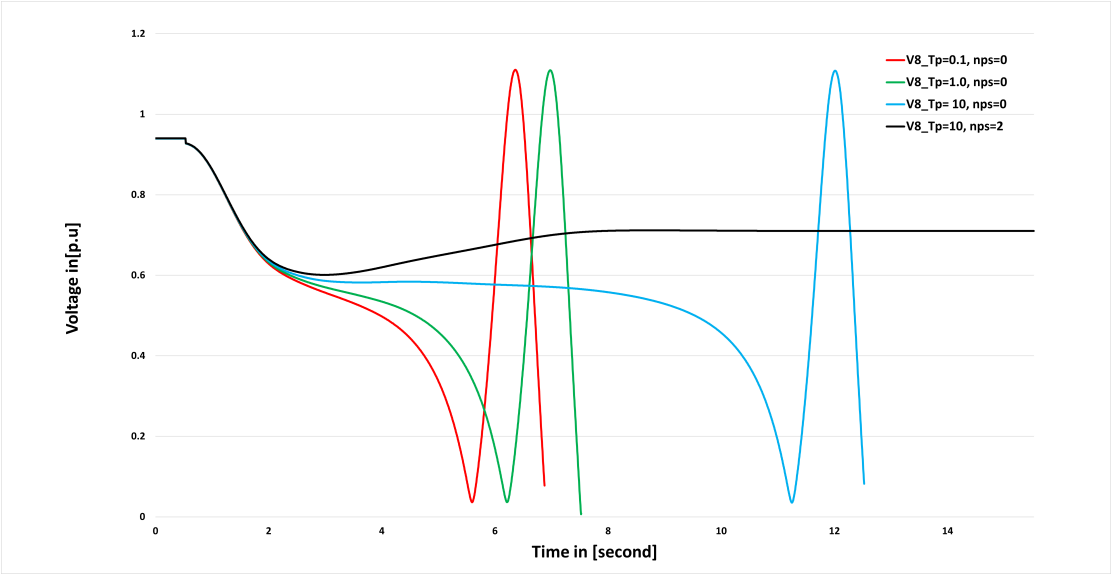

FIGURE 4.9: Case 2: when two lines were disconnected in Kundur Two Area System, L-7-8-1 and L-8-9-1. Voltage magnitude at Bus 8 was collapsed drops to zero. When the steady-state load exponent is equals to zero, transient load exponent equal to two and recovery time constant were varied [0.1, 1.0 and 10]. Solid black line refers to the constant resistive load model, ie. nps=2 npt=2

From the simulation results, we observe that when the steady-state load exponent was zero, $nps = 0$, the voltage magnitude at most loaded area was dropped and oscillated rapidly beyond the limitation. This indicated that the system reached its reactive demand, as a result the system was collapsing. Area 1 and Area 2 were splitted and the rotor angle of the generators was rising. Where the steady-state load exponent was set to two, nps=2, it implies CRL model. In this model, the voltage magnitude at Bus 8 was decreased slowly and it reached stable condition, which was almost 0.24 p.u below the initial voltage magnitude as shown in Figure 4.9. There was not a voltage collapse and the system was stabilized in new equilibrium condition. This is reflecting that the voltage magnitude of CRL model did not depend on the values of recovery time constant. Thus, this load model did not depend on the recovery time constant, only if the steady-state load exponent and the transient load exponents were equal values. Mathematically, the desired output power of the resistive load model has an input only from the transient state as a function of voltage, P_t. The transfer function of the model product was zero. Because both the steady-state power and transient power have equal values, they cancel each other. Thus, the desired output power of CRL model was depending on the transient power, $P_d = P_t$. This refers to static load model.

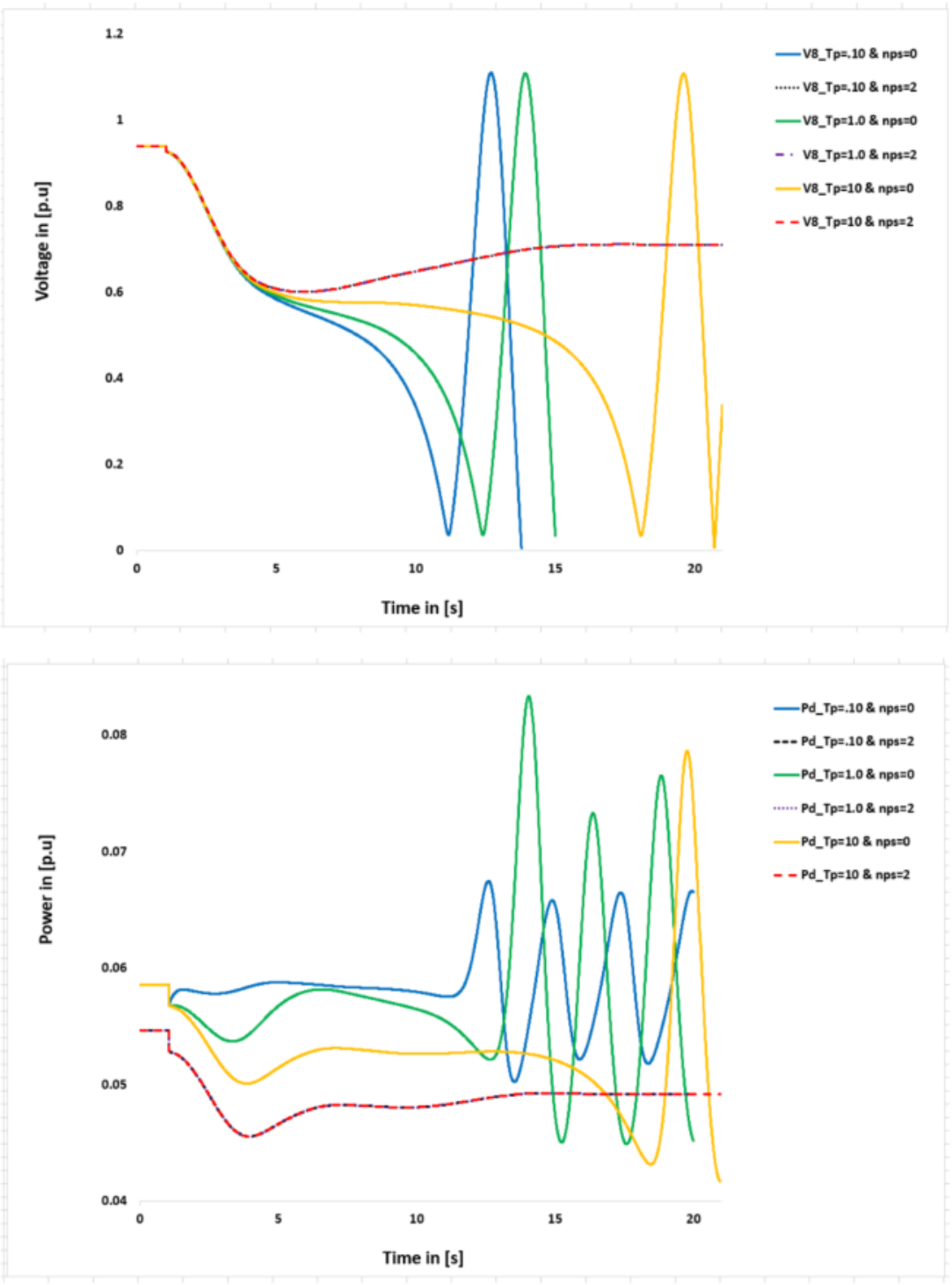

FIGURE 4.10: Case 2: Two lines were disconnected in Kundur Two Area System, which is L-7-8-1 and L-8-9-1. then compare the voltage magnitude at bus 8 when the steady-state load exponent were set zero and two, ie. nps=0 and nps=2, while the transient load exponent was set two, npt=2. And recovery time constant was set ten, Tp=10.

The dynamic load model detected the system disturbance and provided the response regarding the values of the recovery time constant parameters. Thus, the smallest T_p

in our tests equals to 0.1, and the dynamic load model provided a more rapid response than other values of T_p. First disturbance occurred due to the initial input power of the dynamic load model set 0.058 p.u. The system has small oscillation and becomes stable at close the operating point. The main fault in this case was two line outages at 3 seconds, but the simulation result shows only the main part of the simulation. From the simulation results, the desired output power of the dynamic load model varied according to the recovery time constants. Thus, when the recovery time constant was set to small values, the desired output power reached rapidly the initial input power of the dynamic load model. In contrast to small recovery time constant, in large recovery time constant the desired output power was somehow delaying the time of which the instability was presented. It can be shown as in Figure 4.11 that the desired output power of the dynamic load model oscillates, since the system was collapsing. Therefore, the desired power output of the dynamic load model is also depending on the recovery time constant when the steady-state load exponent value was not equal to the transient load exponent. However, the resistive load models did not depend on the recovery time constant and the system was still in stable condition. The desired output power was responding slowly, but it did not reach to the initial input power. The solid black line in Figure 4.11 shows the resistive load model response.

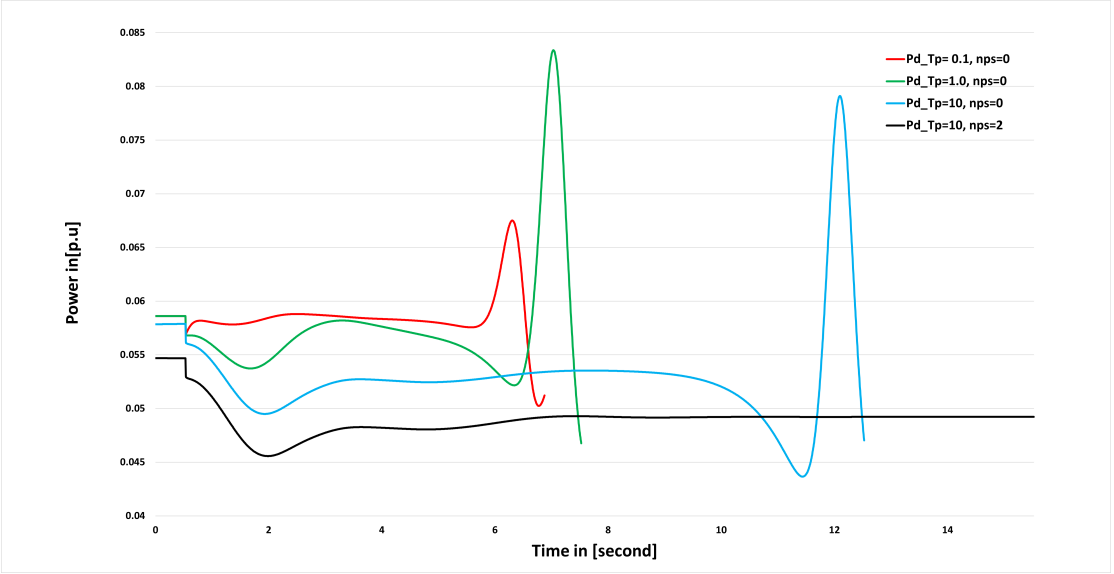

FIGURE 4.11: Case 2: Two line were disconnected in Kundur Two Area System, L-7-8-1 and L-8-9-1. The dynamic load model were response in different scales. The desired output of power depends on the parameter of the dynamic load model, such as nps, npt, and Tp. In this case both the steady-state load exponent and transient exponent are constant values zero and two, respectively, while the recovery time constant were varied [0.1, 1.0and 10]. Whereas, the solid black line refers load flow of the constant resistive load model was applied in the system

The load flow on the remaining transmission line becomes overloaded, which is L-7-8-2 and L-8-9-2. It was almost double compared to the pre-fault condition, especially when the recovery time constant was selected as a large value. This is reflecting that all the transferred power from Area 1 to Area 2 flows through the remaining transmission line. Figure 4.12 shows that the line-outages occurred at 3 seconds. As a result, the simulation of the solid blue color, $T_p = 10$, was oscillated later since the recovery time constant was larger than for the solid red and green color, $T_p = 0.1$ and $T_p = 1.0$, respectively.

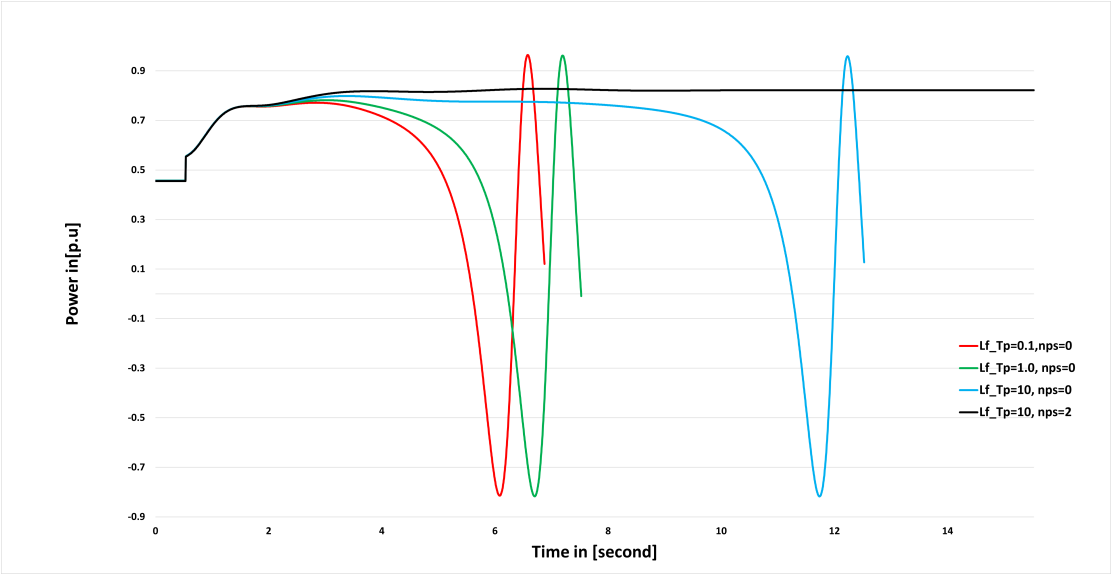

FIGURE 4.12: Case 2: Two transmission lines were disconnected in Kundur Two Area System, L-7-8-1 and L-8-9-1. The load flow across the remaining transmission line, L-7-8-2 and L-8-9-2, were double and oscillated. The steady-state load exponent was equal to zero, the transient load exponent was two and the recovery time constant were varies [0.1, 1.0 and 10]. Whereas, the solid black line refers load flow of the constant resistive load model was applied in the system.

4.3.3 Case 3: Impact of Load Models on the Damping and Power Oscillation

In this case we consider that the entire load of the Nordic 44 network will be replaced with either constant power load model, constant current load model, constant impedance load model or dynamic load model as presented in Table 4.4. All generators connected to an AC interconnected transmission system are synchronous with each other at the same frequency, 50 [Hz]. Due to the gradual reducing of the entire load in the system and gradually rising the load models in the system, immediately following a system disturbance, the generators begin to oscillate relative to each other, causing fluctuations in the system frequency, line loading and system voltages. During the transition of load models, there were oscillations and the frequency variations were approached or near to the nominal frequency. Since these changes are small disturbances, they can not cause loss of synchronism unless the system is operating at, or very near, its steady-state stability limit.

The entire load in Nordic 44 system was represented by CRL Z as shown in the Appendix [A]. It should also be replaced with a CRL model, ie Z_{new}. The main idea is to change the load in the system so that the load characteristics are changing from season to season, weekdays to week-ends and from hour to hour. Moreover, today's demand system was dominated by CPLs, such as electric vehicles, Tv, computers etc. In Nordic countries, most types of loads are CPL model in summer times, while in winter times resistive load dominate the demand. To compare which of these models were worst or best damping, the comparison should begin in the same level of the initial operating point. Therefore, replacing of load process was applied in the beginning of the simulation and their duration was 150 seconds in this case.

TABLE 4.4: Type of load Models

Types of load models	N_{ps}	N_{pt}
Constant Power load model	0	0
Constant Current load model	1	1
Constant Resistive load model	2	2
Dynamic load model	0	2

Figure 4.13 presents the load replacing the load system into the designed load model that is used in this thesis. It presents only the first few seconds of the simulation shown in the plot. From this simulation it was observed that the solid black color refers to CPL, which was a small damping of oscillation compared with other models. In the beginning, there was a fluctuating of the generator speed, but the system was stable after some seconds in all replacing models, either above or below the near operating point. At 60 seconds of the simulation, different load models were almost equal frequency. Thus, the events were applied at 60 seconds in this case. There are many factors contributing to the system losing its synchronism, such as short circuit, line outage or load change. From those events, a short circuit happens often from time to time and these are cleared rather quickly. The fault duration time was the major factor in determining the system stability.

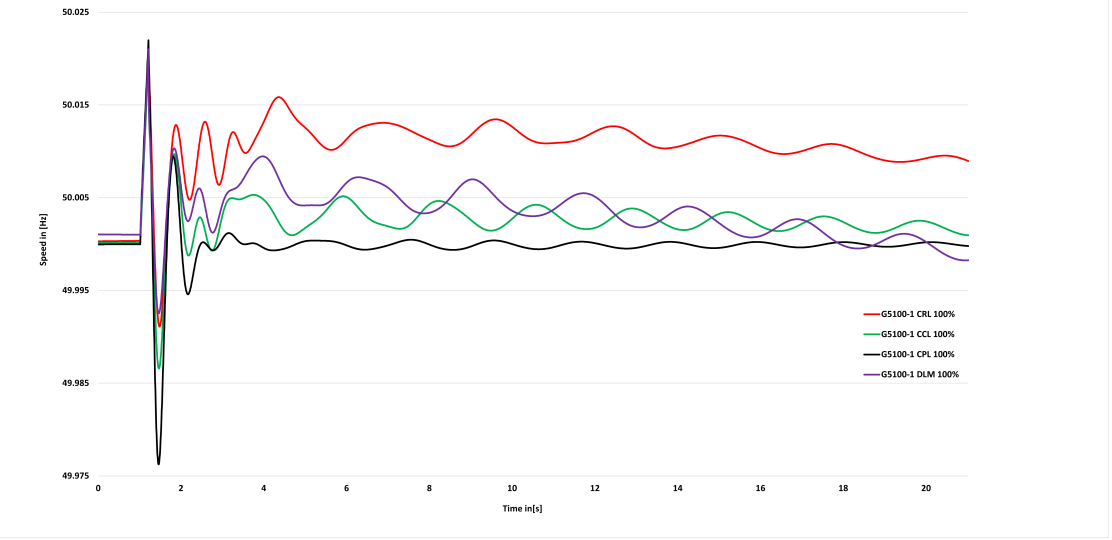

FIGURE 4.13: The entire load of the system will be replaced by the load models. Where, CPL represents for Constant Power Load Model, CCL- Constant Current Load Model, CRL - Constant Resistive Load Model and DLM- Dynamic Load Mode nps=0npt=2, solid green, black, red and blue color line, respectively. There is a small fluctuation in the system and different damping of oscillation.

Different load models have varied critical clearing time based on the system stability, as obtained from the simulation result by trial and error analysis of the system in DynPSSimpy software. The critical clearing time, CCT, is defined as the maximum time interval by which the fault must be cleared in order to preserve the system stability. In other words, CCT is the time when the rotor would have moved to the critical clearing angle. If the clearing time of the fault is beyond the critical clearing time the system will be unstable. Figure 4.14 shows that different clearing time has different oscillation, and the voltage system becomes only oscillated when the clearing time is below CCT, for example 50ms and 200ms. On the other hand, if the clearing time is 300 ms or beyond the CCT, the voltage system collapses. Therefore, the total time duration by the fault should be less than the CCT for stable operation of the system. The CCT lies obviously in between 200ms and 300ms. It is assumed that 200ms of the clearing time would be used in the case of all models, ie. 10 cycles. This helps to check which load model would be higher damping or less.

FIGURE 4.14: Impact of clearing time on voltage stability at Bus 3359. A short circuit is applied at Bus 5100 and the fault duration were lasting 50ms,200ms and 300ms, represent in black dashed, solid green and solid red, respectively.

Table 4.5 summarizes critical clearing time obtained for the system with different load models. Those values are the maximum fault duration for which the system remains transiently stable. This is reflecting that CPL has higher CCT than the CRL. Because the load is not dependent on the voltage in CPLM, it is a constant load. As the voltage decreases due to the fault, the power load is kept constant when the reactive current in the system is increasing. The negative incremental resistance instability of CPLs can cause the voltage to collapse or the system to oscillate by small signal stability problems. Thus, the CCT takes longer in CPL as compared to other models. Whereas, load in CRL is depending on the voltage squared so that it has very short CCT. When the voltage decreased in the CRL, it might lead to transient instabilities or rapid voltage collapse.

TABLE 4.5: Critical clearing time of load Models

Types of load models	Critical clearing time
Constant Resistive load model	210ms
Constant Current load model	270ms
Constant Power load model	255ms
Dynamic load model at Nps =0 & npt =2	205ms

In order to show the effect of the load model on damping of the oscillation system, different load models are replaced in the Nordic 44. The load exponents *nps*and *npt* will be altered for each simulation in order to see how the damping in the system get affected by the different characteristics. The areas vulnerable to voltage collapse or the critical loads can be identified with participation factors. Eigenvector is not as effective as the participation factor, as demonstrated by the results of varying the load parameters. Participation factors reveals that generator G3359-1 contributes the most to this poor damped oscillation mode. Even though, these eigenvalues lie in the LHP (left hand plane) and correspond to oscillatory stable modes. Eigenvalues analysis approach is used to evaluate the power oscillation $\lambda = \alpha + j\beta$ and it was obtained from the participation factor, using those Equation 4.4 and 4.3, to evaluate the damping ratio and frequency of oscillation, respectively.

$$\omega_0 = \frac{\beta}{\pi} \tag{4.3}$$

$$\xi = \frac{-\alpha}{\sqrt{\alpha^2 + \beta^2}} \tag{4.4}$$

Different models are represented in Table 4.6, to compare those models after the short circuit was applied in the system. From the simulation results in Figure 4.15, it turns out that a CPL has shorter oscillation than the other load models. It is clearly seen

TABLE 4.6: Generator 3359-1, Eigenvalues, natural frequency and damping for electro-mechanical modes.

Load Model	Nps	Npt	Eigenvalue $\alpha + j\beta$	Nat.freq ω_0 $[\frac{rad}{sec}]$	$[Hz]$	rel.damping ξ	Percentage %
CPL	0	0	-1.11+j8.4	8.4	1.3369	0.1310	13.10 %
DLM1	0	1	-1.1+j8.4 1	8.41	1.3385	0.1297	12.97 %
DLM2	0	2	-1.02+j8.69	8.69	1.3831	0.1166	11.66 %
DLM3	1	0	-1.11+j8.4	8.4	1.3369	0.1310	13.10 %
CCL	1	1	-1.07+j8.53	8.53	1.3576	0.1245	12.45 %
DLM4	1	2	-0.996+j8.57	8.57	1.3639	0.11544	11.54 %
DLM5	2	0	-1.11+j8.4	8.4	1.3369	0.1310	13.10 %
DLM6	2	1	-1.06+j8.55	8.55	1.3608	0.1230	12.30 %
CRL	2	2	-1.03+j8.6	8.6	1.3687	0.1189	11.89 %

that the load model has a great effect on the speed responses, and CPL has a larger damping ratio as compare with the CRL or other models. This model is invariant and allows loads with a stiff voltage characteristics $n_{ps} = n_{pt} = 0$ to be represented. From this model, it is observed that replacing the loads with CPL worsens the response of the system oscillation. Whereas, the CRL has a low damping ratio and high oscillation. Therefore, the stability of the power system for changes in dynamic load parameters is determined by comparison. Depending on the load parameters, damping might be worse or best.

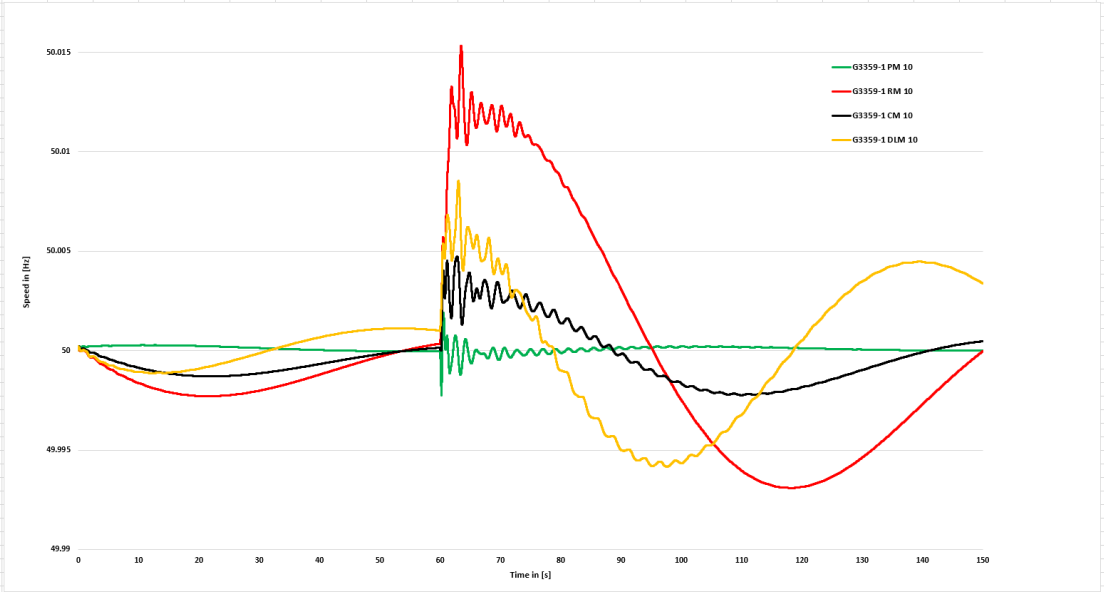

FIGURE 4.15: Impact of different load model in speed response in system. A short circuit is applied at Bus 5100 and the fault duration was lasting 10 cycles

Figure 4.16 and 4.17 represent the speed response and the voltage variation due to the impact of the percentage of CPL in the system, respectively. This was chosen to study the effect of CPLs on the system when the short circuit was applied into the system. Percentages of CPLs were zero, quarter, half and full in the system, and the rest were represented in the network CRLs. These 4 scenarios were simulated in 0%, 25%, 50% and 100 % of CPL. In the first transition period, the speed of the generators oscillated higher in 100% CPL. After a couple of seconds the system was returned to equilibrium point faster when CPL was 100%. From the simulation it is observed that when the percentage of the CPL increased gradually from 0% to 100%, the system was closer to the initial operating point. The results indicate that for a larger percentage of CPL, there is a larger stability margin in the system. As mentioned previously, the voltage dips on the CPL was a worse case than the others. When the percentage of the CPL increased in the load system, it was difficult to control the voltage drops, because the load power was constant and independent on the voltage. Actually, the CCL is unnecessary as it is nearly equivalent to 50 percent CRL combined with 50 percent CPL, as shown in Figure 4.18 and 4.19. It has been found convenient to retain the CCL as it is simple to understand and is frequently used in the absence of more complete data. It is interesting that CCL can be represented by a combination of CRL and CPL with adequate accuracy because this simplifies the load representation.

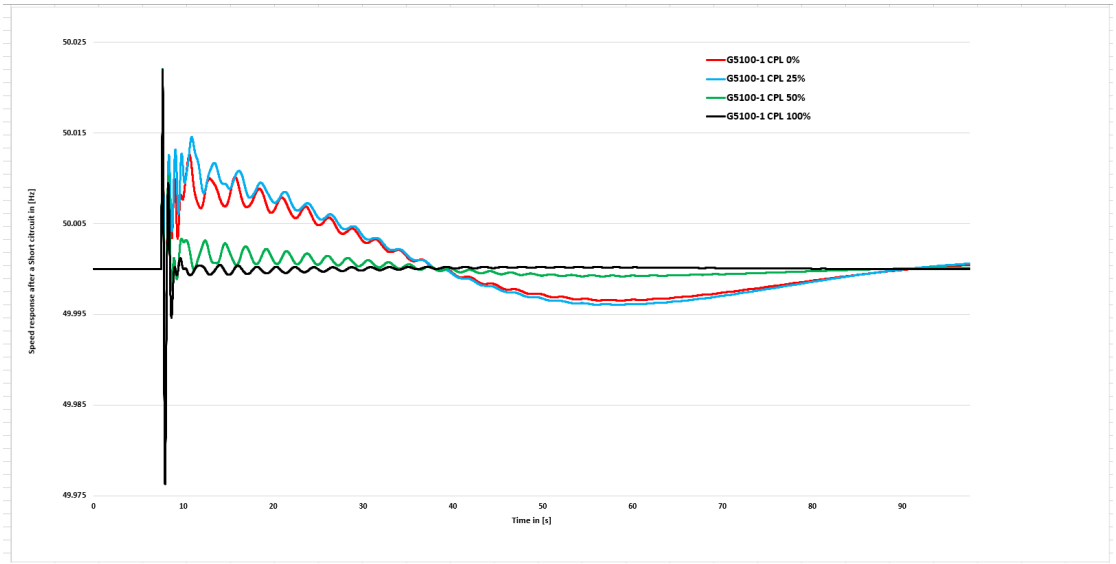

FIGURE 4.16: Impact of increasing constant power load model percentage in Speed response after a short circuit is applied at Bus 5100 and the fault duration was lasting 10 cycles. Solid black, green, blue and red colors refers to zero, quarter, half and full percentage of the constant power load in the system.

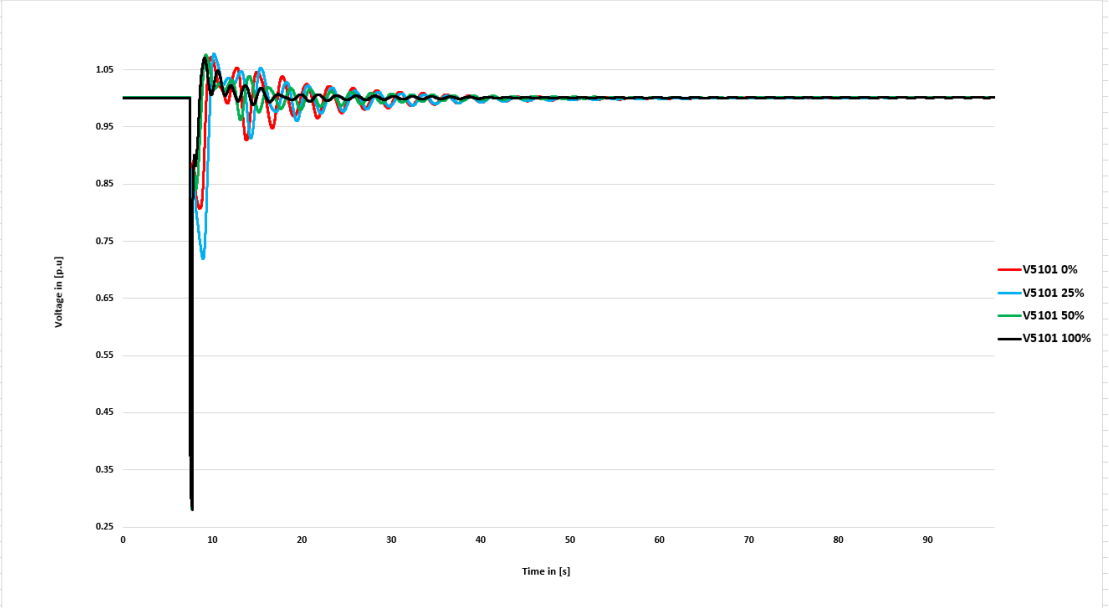

FIGURE 4.17: Impact of increasing constant power load model percentage in Voltage variation after a short circuit is applied at Bus 5100 and the fault duration was lasting 10 cycles. Solid black, green, blue and red colors refers to zero, quarter, half and full percentage of the constant power load in the system

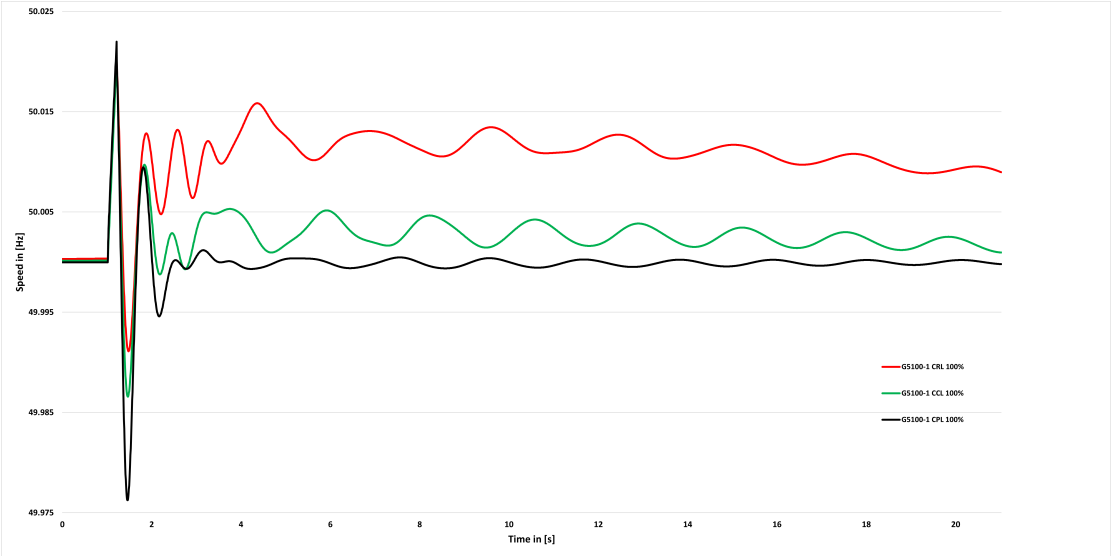

FIGURE 4.18: Impact of load model on power oscillation after a short circuit is applied at Bus 5100 and the fault duration was lasting 10 cycles. Solid black, green, blue and red colors refers to CPL, CCL and CRL 100 percent, respectively, of the entire load in the system

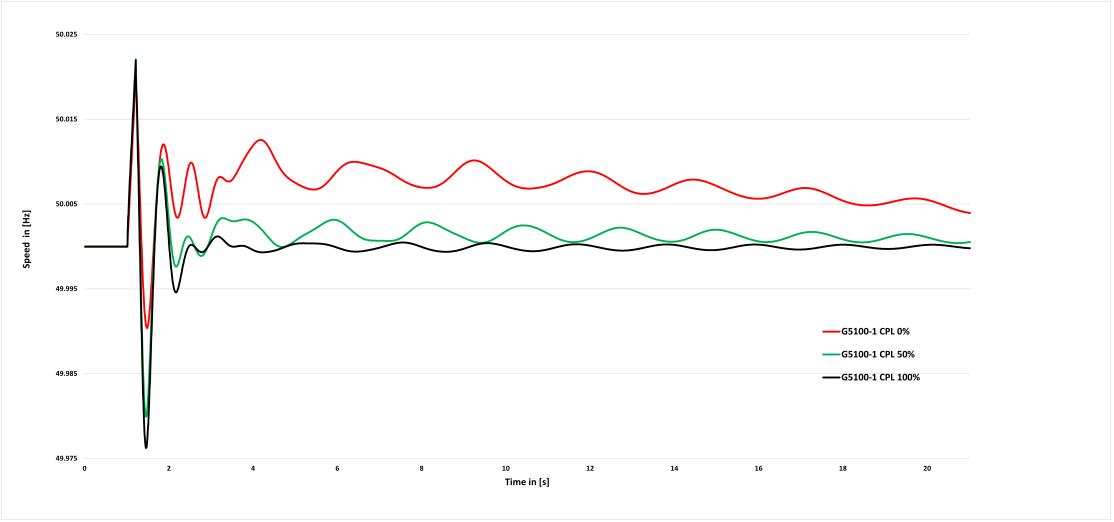

FIGURE 4.19: Impact of load model on power oscillation after a short circuit is applied at Bus 5100 and the fault duration was lasting 10 cycles. Solid black, green, blue and red colors refers to 0% CPL, 50% CPL and 100% CPL, respectively, of the entire load in the system

Changing the entire load in the system with different percentages of CPL had a fluctuation on the power transfer. It was presented in the Figure 4.20 that the load flow from Hasle Bus 5101 in Norway to Ringshal Bus 3359 in Sweden was constant When there was 100% CPL in the system. Whereas, a combination of different load models had a fluctuation in the transfer of power from one station to the other station. Observing that the increasing of CPLs in the system had a detrimental effect on the voltage stability. As a consequence, fast reactive power compensation will increase the power transfer capability of the power system and can, in this sense, help increase the robustness. Besides, it helps the stability margins of the power system.

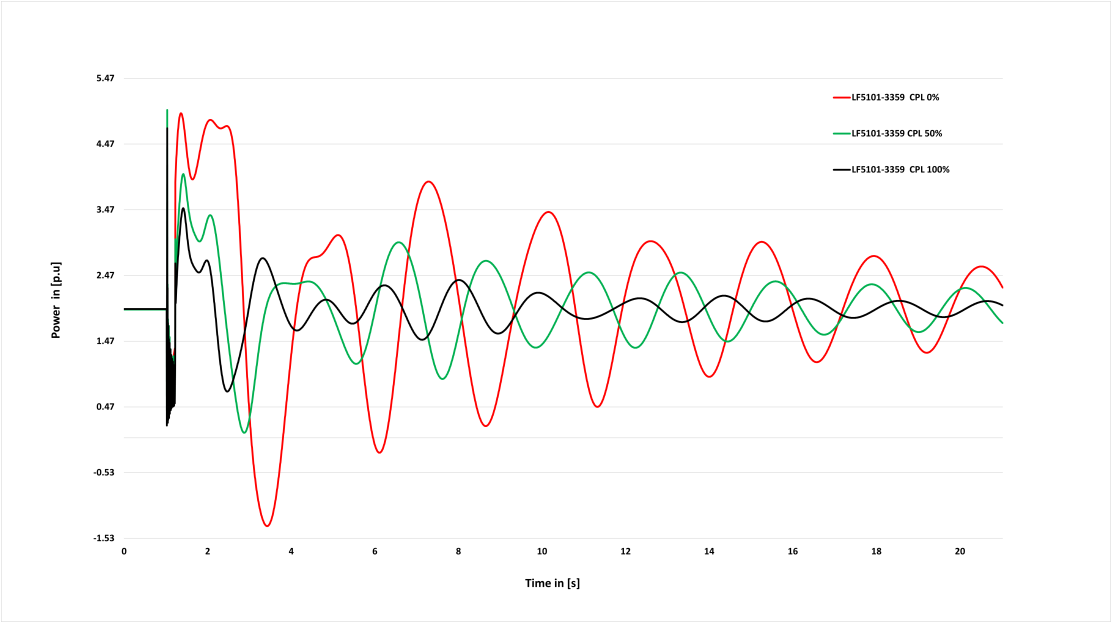

FIGURE 4.20: Impact of increasing constant power load model percentage in load flow from Bus 5101 to Bus 3359 after a short circuit is applied at Bus 5100 and the fault duration was lasting 10 cycles.

From this simulation it is observed that the system was affected by replacing with CPL. This is reflecting that as the percentage of penetration increases, there is a worse response of the system to restore the voltage. Moreover, this is related to the low sensitivity of these loads and there is a greater amount of fixed power. As the voltage gradually decreases there is a huge amount of current flow through the transmission line. If the step voltage occurred in the system, this model is more difficult to return the voltage to its original state.

Both voltage recovery and load recovery of dynamic load model are depend on the load exponents and recovery time constant. As aforementioned, the recovery constant has a significant issues in the voltage stability, and power response has also influenced by recovery time constant. Here, we used recovery time only Tp=10, and the simulation result shown in Figure 4.21 and 4.22.

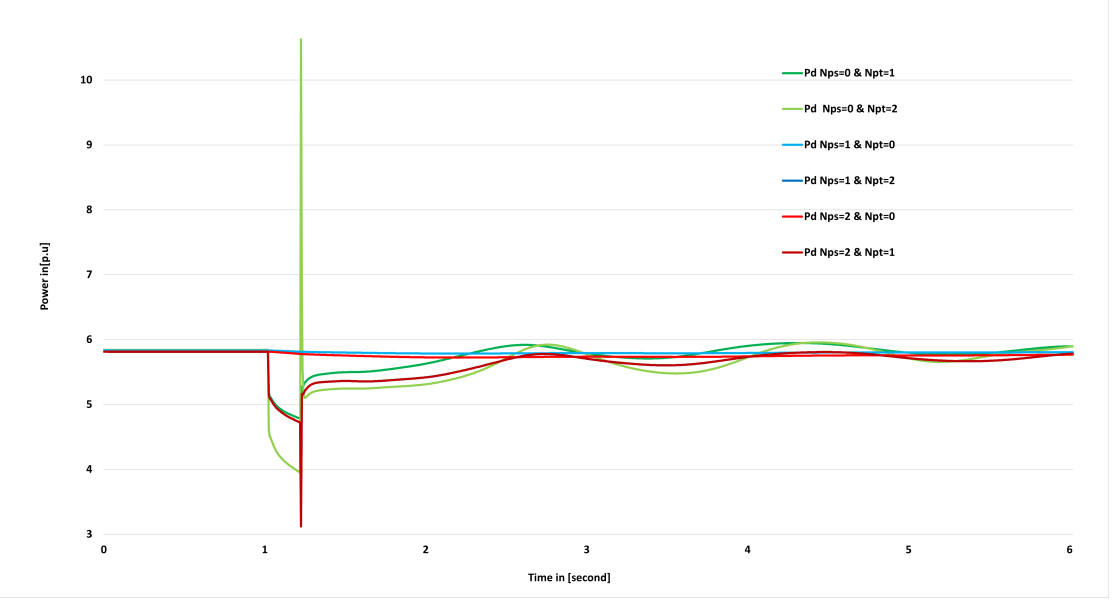

FIGURE 4.21: Load recovery after short circuit was applied in Bus 5100. Different values of load exponents has variety responses such as a converter response when steady-state load exponent was 1 and transient load exponent equals zero.

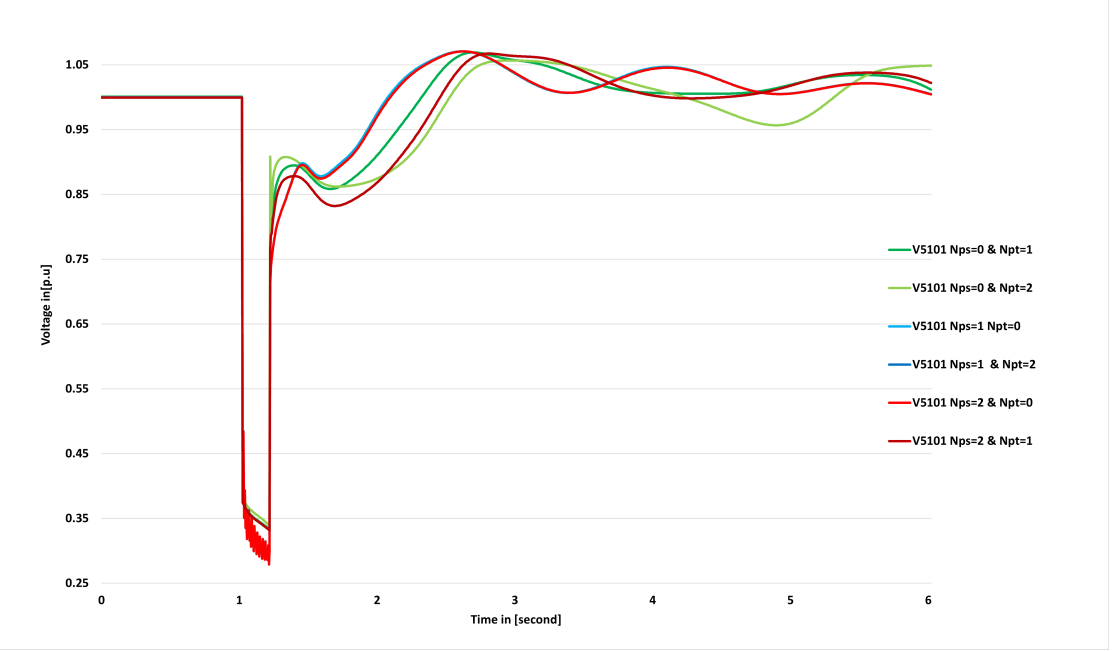

FIGURE 4.22: Voltage recovery after short circuit was applied in Bus 5100. Different values of load exponents has variety responses, for example a converter response when steady-state load exponent and transient load exponent are 1 and 0, respectively, ie.nps=1 npt=zero. Recovery time constant was 10.

4.4 Discussion

This section covers the discussion and summarizes the findings from the results and simulations. The dynamic load model was once again validated by checking how the model responds to a fault in both the Kundur Two Area and the Nordic 44 Test. The Nordic 44 test system is an aggregated model, and by default the load was a CRL. To check the model was working as load-voltage dependence, a short circuit fault was applied in Nordic 44. The load model responses were varied according to the selected load exponents. Therefore, the developed model is an acceptable, simplified representation of the detailed load characteristics. However, certain things should be clarified regarding the simulation results.

The simulation tool used in this thesis is DynPSSimpy. This is one example of open source software. This supports static analysis such as power flow analysis, contingency analysis, etc. and dynamic analysis such as fault analysis, stability analysis, etc. DynPSSimpy contains extensive libraries for generators and their control systems, as well as static and dynamic load models. Working with DynPSSimpy gives you a lot of freedom. This allows you to implement all the models you might want, without getting caught within the confines of the models implemented in commercial software. It also has the capability to work in graphical user interface (GUI) mode. Furthermore, this software applies the linear analysis tools to find the eigenvalues of matrix A, participation factors, and mode shape.

In this thesis, the impact of load models on voltage stability has been investigated. The frequency dependency of the load is ignored in voltage stability studies because it has little impact. Due to a fault condition, we obtained a step voltage in the system. It deals with the modeling of high-voltage bus load models for use in voltage stability studies. As mentioned, the load models used in this investigation are static and dynamic load models. Both types of load models play a significant role in voltage stability. When the entire load is only constant impedance, there will be no stability issue due to loads. Because the power consumed by the constant impedance type of load decreases with the system voltage, However, constant power load models mostly affected the voltage stability. In this type of load, the total power consumed by the load was constant irrespective of the fluctuation in bus voltage. When the voltage of the system decreases due to a fault or contingency, the CPLs draw more current to keep the load constant. As a result, the additional current drawn from the system increases the system losses and voltage drop in the transmission line, which further decreases the bus voltage. Thus, CPL supports the voltage instability phenomenon. Moreover, the nature of the nonlinear dynamic loading model has been shown to be an important factor in determining voltage

fault dynamics. We observed that the voltage stability of the power system depends not only on the load composition but also on the recovery time constant.

Impact of load model on the power oscillation has been simulated. From the simulation result, the most important characteristic of a CPL is its negative incremental resistance. This indicates that the consumed power remain constant when voltage decreases gradually due to a fault, the load current increases gradually, and vice versa. The negative resistance reduces system damping and can lead to instability or unacceptable oscillation response when a significant of system power is consumed by such CPL. Thus, CPL has a critical damping in system and difficult to find the unstable mode. For the CRL, if the load voltage decreases, then the load current also increases, ie. it has positive incremental resistance relationship. Thus, the importance of the load model uncertainty was considered. to accomplish this, load parameters were randomly adjusted, with damping determined for each set of load exponents. This study indicated that the predicted damping levels might have a broad range. It was shown that dynamic load modes might not only impact the damping of electromagnetic modes, but also which generators participated in the mode. This participation may fluctuate as the load characteristics change.

Chapter 5

Conclusion

This chapter contains the primary study outcomes, as well as development and implementation of a dynamic load model and real-time simulation, together with dynamic simulations conducted in Python. This thesis has illustrate the study of voltage stability performance obtained by accurate dynamic load model. It is critical that the power system operators grasp power system stability concepts. Despite the fact that teaching power system is challenging owing to the limited availability of actual network trials, dynamic simulation experiences have proven to be beneficial for new operations in dealing with forthcoming power system management and operational issues. Furthermore, the training simulator is an excellent tool for familiarizing operators with a potentially severe situation. In this thesis, the DynPSSimpy software provides various advantages for operators and researchers. The performance of the installed DLOADs is validated using a series of non-linear simulations that take into account the differential-and algebraic-equations that describe the system's dynamic.

The ultimate goals of this thesis was to produce appropriate dynamic load model for voltage stability studies. Accurate dynamic load models enable more exact estimates of power system controls and stability limits, which are essential in the power systems planning and operation. While inaccurate load modelling could lead to a power system operating in modes that result in actual system collapse or separation. In static load model, where the load is represented as a constant impedance, constant current and constant power, or a combination of these three, are commonly used in current stability and control computer programs. From system stability point of view, the CPL type load representation is the most severe representation. Because of its effect in amplifying voltage oscillations, a drop in voltage will cause an increase in load current resulting in further voltage drop. Conversely, CRL s have a decided damping effect of voltage oscillations. These static load models are adequate for some types of dynamic analysis,

but not for others. Therefore, it is a strong need to develop an accurate dynamic load model.

Further, since only voltage dependent loads have been used in this thesis, another important issue that will be investigated in the future will be the inclusion of both voltage and frequency dependent load in the power system. With the advent of communication methodologies over the last decade, instrumentation and automatic records are now available which may make it feasible for utilities to obtain load characteristics without test. Further work By installing the PMUs at specific buses, whenever a system disturbance occurs, pertinent data can be recorded and even transmitted to a digital computer for analysis. Thereby, the innovative Digital Twin is one of the most promising concepts as it addresses increasing requirements in terms of dynamic effects, modelling accuracy and operator awareness.

Appendix A

Appendix A

This appendix provides the system data of Nordic 44 test network and Kundur Two Area test network used throughout this thesis.

A.1 Nordic 44 Test

A.1.1 Generator Parameters Nordic 44

The generator data for the Kundur Two Area test network are presented in Table A.1

A.1.2 Transmission Line Parameters Nordic 44

The transmission line data for the Kundur Two Area test network are presented in Table A.2.

A.1.3 Load Parameters Nordic 44

The load data for the Kundur Two Area test network are presented in Table A.3.

A.1.4 Transformer Parameters Nordic 44

The transformer data for the Kundur Two Area test network are presented in Table A.4.

Table A.1: Generator Parameter Nordic 44

name	bus	Sn	Vn	P	V	H	D	Xd	Xq	Xdt	Xqt	Xdst	Xqst	Td0t	Tq0t	Td0st	Tq0st
G3000-1	3000	1300	0	550	1	5.97	0	2.22	2.13	0.36	0.468	0.225	0.225	5	1	0.05	0.05
G3000-2	3000	1300	0	550	1	5.97	0	2.22	2.13	0.36	0.468	0.225	0.225	5	1	0.05	0.05
G3000-3	3000	1300	0	0	1	5.97	0	2.22	2.13	0.36	0.468	0.225	0.225	5	1	0.05	0.05
G3115-1	3115	1450.62	0	1175	1	4.741	0	0.946	0.565	0.29	0.565	0.23	0.23	7.57	1	0.045	0.1
G3115-2	3115	1450.62	0	1175	1	4.741	0	0.946	0.565	0.29	0.565	0.23	0.23	7.57	1	0.045	0.1
G3115-3	3115	1450.62	0	1175	1	4.741	0	0.946	0.565	0.29	0.565	0.23	0.23	7.57	1	0.045	0.1
G3245-1	3245	1234.57	0	1000	1	3.3	0	0.75	0.5	0.25	0.5	0.15385	0.15385	5	1	0.06	0.1
G3249-1	3249	1357	0	1042	1	4.543	0	1.036	0.63	0.28	0.63	0.21	0.21	10.13	1	0.06	0.1
G3249-2	3249	1357	0	1042	1	4.543	0	1.036	0.63	0.28	0.63	0.21	0.21	10.13	1	0.06	0.1
G3249-3	3249	1357	0	1042	1	4.543	0	1.036	0.63	0.28	0.63	0.21	0.21	10.13	1	0.06	0.1
G3249-4	3249	1357	0	1042	1	4.543	0	1.036	0.63	0.28	0.63	0.21	0.21	10.13	1	0.06	0.1
G3249-5	3249	1357	0	1042	1	4.543	0	1.036	0.63	0.28	0.63	0.21	0.21	10.13	1	0.06	0.1
G3249-6	3249	1357	0	1042	1	4.543	0	1.036	0.63	0.28	0.63	0.21	0.21	10.13	1	0.06	0.1
G3249-7	3249	1357	0	1042	1	4.543	0	1.036	0.63	0.28	0.63	0.21	0.21	10.13	1	0.06	0.1
G3300-1	3300	1100	0	998.734	1	6	0	2.42	2	0.23	0.4108	0.16	0.16	10.8	1	0.05	0.05
G3300-2	3300	1100	0	998.734	1	6	0	2.42	2	0.23	0.4108	0.16	0.16	10.8	1	0.05	0.05
G3300-3	3300	1100	0	998.734	1	6	0	2.42	2	0.23	0.4108	0.16	0.16	10.8	1	0.05	0.05
G3359-1	3359	1350	0	1110	1	4.82	0	2.13	2.03	0.31	0.403	0.1937	0.1937	4.75	1	0.05	0.05
G3359-2	3359	1350	0	1100	1	4.82	0	2.13	2.03	0.31	0.403	0.1937	0.1937	4.75	1	0.05	0.05
G3359-3	3359	1350	0	1100	1	4.82	0	2.13	2.03	0.31	0.403	0.1937	0.1937	4.75	1	0.05	0.05
G3359-4	3359	1350	0	0	1	4.82	0	2.13	2.03	0.31	0.403	0.1937	0.1937	4.75	1	0.05	0.05
G3359-5	3359	1350	0	0	1	4.82	0	2.13	2.03	0.31	0.403	0.1937	0.1937	4.75	1	0.05	0.05
G3359-6	3359	1350	0	0	1	4.82	0	2.13	2.03	0.31	0.403	0.1937	0.1937	4.75	1	0.05	0.05
G5100-1	5100	1200	0	972.437	1	3.9871	0	1.1332	0.68315	0.24302	0.68315	0.15135	0.15135	4.9629	1	0.05	0.15
G5300-1	5300	1574.89	0	1275.661	1	3.5	0	1.14	0.84	0.34	0.84	0.26	0.26	6.4	1	0.05	0.15
G5300-2	5300	1574.89	0	1275.661	1	3.5	0	1.14	0.84	0.34	0.84	0.26	0.26	6.4	1	0.05	0.15
G5400-1	5400	1611.516	0	1305.328	1.007	4.1	0	1.02	0.63	0.25	0.63	0.16	0.16	6.5	1	0.05	0.15
G5400-2	5400	1611.516	0	1305.328	1.007	4.1	0	1.02	0.63	0.25	0.63	0.16	0.16	6.5	1	0.05	0.15
G5500-1	5500	1450	0	1131.563	1.004	3	0	1.2364	0.65567	0.37415	0.65567	0.22825	0.22825	7.198	1	0.05	0.15
G5600-1	5600	1538.265	0	1245.995	1.01	3.5	0	1	0.51325	0.38	0.51325	0.28	0.28	7.85	1	0.05	0.15
G5600-2	5600	1538.265	0	1245.995	1.01	3.5	0	1	0.51325	0.38	0.51325	0.28	0.28	7.85	1	0.05	0.15
G6000-1	6000	896.59	0	735.73	1.005	3.5	0	1.28	0.94	0.37	0.94	0.28	0.28	9.7	1	0.05	0.15
G6100-1	6100	1634.96	0	1329.061	1	3	0	1.2	0.73	0.37	0.73	0.18	0.18	9.9	1	0.05	0.15
G6100-2	6100	1634.96	0	1329.061	1	3	0	1.2	0.73	0.37	0.73	0.18	0.18	9.9	1	0.05	0.15
G6100-3	6100	1634.96	0	1329.061	1	3	0	1.2	0.73	0.37	0.73	0.18	0.18	9.9	1	0.05	0.15
G6100-4	6100	1634.96	0	1329.061	1	3	0	1.2	0.73	0.37	0.73	0.18	0.18	9.9	1	0.05	0.15
G6100-5	6100	1634.96	0	1329.061	1	3	0	1.2	0.73	0.37	0.73	0.18	0.18	9.9	1	0.05	0.15
G6500-1	6500	1100	0	814.333	1	3.558	0	1.0679	0.642	0.23865	0.642	0.15802	0.15802	5.4855	1	0.05	0.15
G6500-2	6500	1100	0	814.333	1	3.558	0	1.0679	0.642	0.23865	0.642	0.15802	0.15802	5.4855	1	0.05	0.15
G6500-3	6500	1100	0	814.333	1	3.558	0	1.0679	0.642	0.23865	0.642	0.15802	0.15802	5.4855	1	0.05	0.15
G6500-4	6500	1100	0	0	1	3.558	0	1.0679	0.642	0.23865	0.642	0.15802	0.15802	5.4855	1	0.05	0.15
G6700-1	6700	2144.444	0	1753	1.02	3.592	0	1.1044	0.66186	0.25484	0.66186	0.17062	0.17062	5.24	1	0.05	0.15
G6700-2	6700	2144.444	0	1753	1.02	3.592	0	1.1044	0.66186	0.25484	0.66186	0.17062	0.17062	5.24	1	0.05	0.15
G7000-1	7000	1278	0	1085.5	1	5.5	0	2.22	2.13	0.36	0.468	0.225	0.225	10	1	0.05	0.05
G7000-2	7000	1278	0	1085.5	1	5.5	0	2.22	2.13	0.36	0.468	0.225	0.225	10	1	0.05	0.05
G7000-3	7000	1278	0	1085.5	1	5.5	0	2.22	2.13	0.36	0.468	0.225	0.225	10	1	0.05	0.05
G7000-4	7000	1278	0	1085.5	1	5.5	0	2.22	2.13	0.36	0.468	0.225	0.225	10	1	0.05	0.05
G7000-5	7000	1278	0	1085.5	1	5.5	0	2.22	2.13	0.36	0.468	0.225	0.225	10	1	0.05	0.05
G7000-6	7000	1278	0	1085.5	1	5.5	0	2.22	2.13	0.36	0.468	0.225	0.225	10	1	0.05	0.05
G7000-7	7000	1278	0	0	1	5.5	0	2.22	2.13	0.36	0.468	0.225	0.225	10	1	0.05	0.05
G7000-8	7000	1278	0	0	1	5.5	0	2.22	2.13	0.36	0.468	0.225	0.225	10	1	0.05	0.05
G7000-9	7000	1278	0	0	1	5.5	0	2.22	2.13	0.36	0.468	0.225	0.225	10	1	0.05	0.05
G7100-1	7100	1000	0	715.333	1	3.2	0	0.75	0.5	0.25	0.5	0.15385	0.15385	5	1	0.06	0.1
G7100-2	7100	1000	0	715.333	1	3.2	0	0.75	0.5	0.25	0.5	0.15385	0.15385	5	1	0.06	0.1
G7100-3	7100	1000	0	715.333	1	3.2	0	0.75	0.5	0.25	0.5	0.15385	0.15385	5	1	0.06	0.1
G8500-1	8500	1300	0	994	1.02	7	0	2.42	2	0.23	0.4108	0.17062	0.17062	10	1	0.05	0.05
G8500-2	8500	1300	0	0	1.02	7	0	2.42	2	0.23	0.4108	0.17062	0.17062	10	1	0.05	0.05
G8500-3	8500	1300	0	0	1.02	7	0	2.42	2	0.23	0.4108	0.17062	0.17062	10	1	0.05	0.05
G8500-4	8500	1300	0	0	1.02	7	0	2.42	2	0.23	0.4108	0.17062	0.17062	10	1	0.05	0.05
G8500-5	8500	1300	0	0	1.02	7	0	2.42	2	0.23	0.4108	0.17062	0.17062	10	1	0.05	0.05
G8500-6	8500	1300	0	0	1.02	7	0	2.42	2	0.23	0.4108	0.17062	0.17062	10	1	0.05	0.05

Table A.2: Transmission Line Parameter Nordic 44

Name	from_bus	To_bus	length	Sn	Vn	units	R	X	B
L3000-3020	3000	3020	1	0	0	p.u.	0	0.006	0
L3000-3115	3000	3115	1	0	0	p.u.	0.045	0.54	0.5
L3000-3245	3000	3245	1	0	0	p.u.	0.0048	0.072	0.05
L3000-3245	3000	3245	1	0	0	p.u.	0.0108	0.12	0.05
L3000-3300	3000	3300	1	0	0	p.u.	0.0036	0.048	0.03
L3000-3300	3000	3300	1	0	0	p.u.	0.0054	0.06	0.025
L3100-3115	3100	3115	1	0	0	p.u.	0.018	0.24	0.11
L3100-3200	3100	3200	1	0	0	p.u.	0.024	0.144	0.2
L3100-3200	3100	3200	1	0	0	p.u.	0.024	0.144	0.2
L3100-3200	3100	3200	1	0	0	p.u.	0.024	0.144	0.2
L3100-3249	3100	3249	1	0	0	p.u.	0.018	0.258	0.16
L3100-3359	3100	3359	1	0	0	p.u.	0.048	0.3	0.25
L3100-3359	3100	3359	1	0	0	p.u.	0.024	0.138	0.24
L3115-3245	3115	3245	1	0	0	p.u.	0.027	0.3	0.14
L3115-3249	3115	3249	1	0	0	p.u.	0.009	0.12	0.08
L3115-6701	3115	6701	1	0	0	p.u.	0.024	0.24	0.1
L3115-7100	3115	7100	1	0	0	p.u.	0.024	0.078	0.13
L3200-3300	3200	3300	1	0	0	p.u.	0.012	0.12	0.06
L3200-3359	3200	3359	1	0	0	p.u.	0.006	0.12	0.07
L3200-8500	3200	8500	1	0	0	p.u.	0.006	0.102	0.06
L3244-6500	3244	6500	1	0	0	p.u.	0.006	0.12	0.06
L3249-7100	3249	7100	1	0	0	p.u.	0.012	0.045	0.078
L3300-8500	3300	8500	1	0	0	p.u.	0.012	0.138	0.06
L3300-8500	3300	8500	1	0	0	p.u.	0.0072	0.162	0.1
L3359-5101-1	3359	5101	1	0	0	p.u.	0.0096	0.156	0.09
L3359-5101-2	3359	5101	1	0	0	p.u.	0.012	0.132	0.06
L3359-8500	3359	8500	1	0	0	p.u.	0.0072	0.162	0.1
L3359-8500	3359	8500	1	0	0	p.u.	0.015	0.192	0.09
L3701-6700	3701	6700	1	0	0	p.u.	0.15	1.2	0.03
L5100-5500	5100	5500	1	0	0	p.u.	0.0162	0.156	0.044
L5100-6500	5100	6500	1	0	0	p.u.	0.048	0.54	0.06
L5101-5102	5101	5102	1	0	0	p.u.	0.0048	0.06	0.09
L5101-5103	5101	5103	1	0	0	p.u.	0.006	0.084	0.04
L5101-5501	5101	5501	1	0	0	p.u.	0.006	0.09	0.55
L5102-5103	5102	5103	1	0	0	p.u.	0.0024	0.042	0.03
L5102-5304	5102	5304	1	0	0	p.u.	0.0102	0.144	0.07
L5102-6001	5102	6001	1	0	0	p.u.	0.018	0.276	0.13
L5103-5304	5103	5304	1	0	0	p.u.	0.012	0.15	0.07
L5103-5304	5103	5304	1	0	0	p.u.	0.0078	0.12	0.06
L5300-6100	5300	6100	1	0	0	p.u.	0.0126	0.132	0.01
L5301-5304	5301	5304	1	0	0	p.u.	0.006	0.12	0.06
L5301-5305	5301	5305	1	0	0	p.u.	0.0042	0.072	0.031
L5301-6001	5301	6001	1	0	0	p.u.	0.0078	0.12	0.05
L5304-5305	5304	5305	1	0	0	p.u.	0.006	0.09	0.05
L5304-5305	5304	5305	1	0	0	p.u.	0.0078	0.0102	0.04
L5400-5500	5400	5500	1	0	0	p.u.	0.0054	0.564	0.05
L5400-6000	5400	6000	1	0	0	p.u.	0.0198	0.216	0.025
L5401-5501	5401	5501	1	0	0	p.u.	0.0105	0.162	0.08
L5401-5602	5401	5602	1	0	0	p.u.	0.0096	0.153	0.09
L5401-6001	5401	6001	1	0	0	p.u.	0.00384	0.06	0.028
L5402-6001	5402	6001	1	0	0	p.u.	0.00042	0.006	0.003
L5500-5603	5500	5603	1	0	0	p.u.	0.03	0.36	0.05
L5600-5601	5600	5601	1	0	0	p.u.	0.018	0.204	0.02
L5600-5603	5600	5603	1	0	0	p.u.	0.012	0.132	0.02
L5600-5620	5600	5620	1	0	0	p.u.	0	0.006	0
L5600-6000	5600	6000	1	0	0	p.u.	0.012	0.12	0.07
L5603-5610	5603	5610	1	0	0	p.u.	0	0.006	0
L6000-6100	6000	6100	1	0	0	p.u.	0.0204	0.252	0.03
L6500-6700	6500	6700	1	0	0	p.u.	0.102	1.08	0.1
L6500-6700	6500	6700	1	0	0	p.u.	0.06	0.78	0.12
L7000-7010	7000	7010	1	0	0	p.u.	0	0.006	0
L7000-7020	7000	7020	1	0	0	p.u.	0	0.006	0
L7000-7100	7000	7100	1	0	0	p.u.	0.024	0.072	0.13
L7000-7100	7000	7100	1	0	0	p.u.	0.024	0.072	0.13
L7000-7100	7000	7100	1	0	0	p.u.	0.024	0.084	0.13
L8500-8600	8500	8600	1	0	0	p.u.	0	0.006	0
L8500-8700	8500	8700	1	0	0	p.u.	0	0.006	0

Table A.3: Loads Parameter Nordic 44

Name	bus	P	Q	Model
L3000-1	3000	1420.656	567	Z
L3000-2	3000	1420.656	567	Z
L3000-3	3000	1420.656	567	Z
L3020-1	3020	1219	616	Z
L3100-1	3100	621	110	Z
L3115-1	3115	621	650	Z
L3249-1	3249	2265	650	Z
L3300-1	3300	1217.358	400	Z
L3300-2	3300	1217.358	400	Z
L3359-1	3359	1460.829	600	Z
L3359-2	3359	1460.829	600	Z
L3359-3	3359	1460.829	600	Z
L3359-4	3359	1460.829	600	Z
L3360-1	3360	-330	262	Z
L5100-1	5100	1154.17	70	Z
L5300-1	5300	2651	-70	Z
L5400-1	5400	1149.765	100	Z
L5500-1	5500	2203.415	200	Z
L5500-2	5500	2203.415	200	Z
L5600-1	5600	674.862	125	Z
L5600-2	5600	674.862	125	Z
L5610-1	5610	1412	363	Z
L5620-1	5620	414	175	Z
L6100-1	6100	1199.755	400	Z
L6100-2	6100	1199.755	400	Z
L6500-1	6500	1013	333	Z
L6500-2	6500	1013	333	Z
L6500-3	6500	1013	333	Z
L6700-1	6700	2489	150	Z
L7000-1	7000	1593.526	70	Z
L7000-2	7000	1593.526	70	Z
L7000-3	7000	1593.526	70	Z
L7000-4	7000	1593.526	70	Z
L7000-5	7000	1593.526	70	Z
L7010-1	7010	-1219	600	Z
L7020-1	7020	343	-4	Z
L7100-1	7100	1431.684	200	Z
L7100-2	7100	1431.684	200	Z
L8500-1	8500	1240	433	Z
L8500-2	8500	1240	433	Z
L8500-3	8500	1240	433	Z
L8600-1	8600	546	10	Z
L8700-1	8700	628	0	Z

TABLE A.4: Transformer Parameter Nordic 44

Name	frm_bus	To_bus	Sn	Vn_from	Vn_to	R	X	Ratio
T3244-3245	3244	3245	1000	0	0	0.005	0.02	1
T3701-3249	3701	3249	1000	0	0	0.02	0.5	1
T3359-3360	3359	3360	1000	0	0	0.005	0.02	1
T5101-5100	5101	5100	1000	0	0	0.0008	0.0305	1
T5300-5301	5300	5301	1000	0	0	0.0016	0.061	1
T5400-5401	5400	5401	1000	0	0	0.0032	0.12	1
T5400-5402	5400	5402	1000	0	0	0.0004	0.015	1
T5500-5501	5500	5501	1000	0	0	0.0004	0.015	1
T5601-6001	5601	6001	1000	0	0	0.0002	0.0076	1
T5603-5602	5603	5602	1000	0	0	0.0008	0.0305	1
T6000-6001	6000	6001	1000	0	0	0.0004	0.015	1
T6700-6701	6700	6701	1000	0	0	0.0005	0.02	1

TABLE A.5: Governor Parameter Nordic 44

Name	Gen	R	Dt	Vmin	Vmax	T2	t3	T4	Pm0	Tw
GOV2	G3000-1	0.05	0	0	1	0.36	6	67.6	0.424	1
GOV3	G3000-2	0.05	0	0	1	0.36	6	67.6	0.424	1
GOV4	G3000-3	0.05	0	0	1	0.36	6	67.6	0.1	1
GOV5	G5400-1	0.05	0	0	1	0.36	6	67.6	0.81	1
GOV6	G5400-2	0.05	0	0	1	0.36	6	67.6	0.81	1
GOV7	G6700-1	0.05	0	0	1	0.36	6	67.6	0.82	1
GOV8	G6700-2	0.05	0	0	1	0.36	6	67.6	0.82	1
GOV9	G7100-1	0.05	0	0	1	0.36	6	67.6	0.715	1
GOV10	G7100-2	0.05	0	0	1	0.36	6	67.6	0.715	1
GOV11	G7100-3	0.05	0	0	1	0.36	6	67.6	0.715	1

A.1.5 Governor Parameters Nordic 44

The governor data for the Kundur Two Area test network are presented in Table A.5.

A.1.6 AVR Parameters Nordic 44

The AVR data for the Kundur Two Area test network are presented in Table A.6.

A.1.7 Dynamic Load Model parameters Nordic 44

The dynamic load model data for the Kundur Two Area test network are presented in Table ??.

Table A.6: AVR Parameter Nordic 44

Name	gen	K	Ta	Tb	Te	Emin	Emax
AVR2	G3000-1	100	2	10	0.5	-3	3
AVR3	G3000-2	100	2	10	0.5	-3	3
AVR4	G3000-3	100	2	10	0.5	-3	3
AVR5	G5400-1	100	2	10	0.5	-3	3
AVR6	G5400-2	100	2	10	0.5	-3	3
AVR7	G6700-1	100	2	10	0.5	-3	3
AVR8	G6700-2	100	2	10	0.5	-3	3
AVR9	G7100-1	100	2	10	0.5	-3	3
AVR10	G7100-2	100	2	10	0.5	-3	3
AVR11	G7100-3	100	2	10	0.5	-3	3
AVR18	G6100-1	100	2	10	0.5	-3	3
AVR19	G6100-2	100	2	10	0.5	-3	3
AVR20	G6100-3	100	2	10	0.5	-3	3
AVR21	G6100-4	100	2	10	0.5	-3	3
AVR22	G6100-5	100	2	10	0.5	-3	3

Table A.7: Dynamic Load Model Parameters Nordic 44

Name	Bus	nps	npt	Tp	P0
Load1	3000	0	2	2	0
Load2	3020	0	2	2	0
Load3	3100	0	2	2	0
Load4	3115	0	2	2	0
Load5	3200	0	2	2	0
Load6	3244	0	2	2	0
Load7	3245	0	2	2	0
Load8	3249	0	2	2	0
Load9	3300	0	2	2	0
Load10	3359	0	2	2	0
Load11	3360	0	2	2	0
Load12	3701	0	2	2	0
Load13	5100	0	2	2	0
Load14	5101	0	2	2	0
Load15	5102	0	2	2	0
Load16	5103	0	2	2	0
Load17	5300	0	2	2	0
Load18	5301	0	2	2	0
Load19	5304	0	2	2	0
Load20	5305	0	2	2	0
Load21	5306	0	2	2	0
Load22	5401	0	2	2	0
Load23	5402	0	2	2	0
Load24	5500	0	2	2	0
Load25	5501	0	2	2	0
Load26	5600	0	2	2	0
Load27	5601	0	2	2	0
Load28	5602	0	2	2	0
Load29	5603	0	2	2	0
Load30	5610	0	2	2	0
Load31	5620	0	2	2	0
Load32	6000	0	2	2	0
Load33	6001	0	2	2	0
Load34	6100	0	2	2	0
Load35	6500	0	2	2	0
Load36	6700	0	2	2	0
Load37	6701	0	2	2	0
Load38	7000	0	2	2	0
Load39	7010	0	2	2	0
Load40	7020	0	2	2	0
Load41	7100	0	2	2	0
Load42	8500	0	2	2	0
Load43	8600	0	2	2	0
Load44	8700	0	2	2	0

Appendix B

Appendix B

B.1 Kundur's Two Area System Parameters

B.1.1 Line Parameter K2A

The line impedance data for the Kundur Two Area for the test network is presented in Table B.1.

B.1.2 Generator Parameters K2A

The generator data for the Kundur Two Area test network are presented in Table B.2.

B.1.3 Transformer Parameters K2A

The transformer data for the Kundur Two Area test network are presented in Table B.3.

Table B.1: Line Parameter K2A

From	To	Length	Sn[MVA]	Vn[kV]	unit	R	X	B
B5	B6	25	100	230	pu	0.0001	0.001	0.00175
B6	B7	10	100	230	pu	0.0001	0.001	0.00175
B7	B8	110	100	230	pu	0.0001	0.001	0.00175
B7	B8	110	100	230	pu	0.0001	0.001	0.00175
B8	B9	110	100	230	pu	0.0001	0.001	0.00175
B8	B9	110	100	230	pu	0.0001	0.001	0.00175
B9	B10	10	100	230	pu	0.0001	0.001	0.00175
B10	B11	25	100	230	pu	0.0001	0.001	0.00175

TABLE B.2: Generator Parameter K2A

Gen	Bus	Sn	Vn	P	V	H	D	Xd	Xq	Xd'	Xq'	Xd"	Xq"	Td0'	Tq0'	Td0"	Tq0"
G1	B1	900	20	700	1.03	7	0	1.2	0.9	0.3	0.55	0.25	0.25	5	0.1	0.03	0.05
G2	B2	900	20	700	1.01	7	0	1.2	0.9	0.3	0.55	0.25	0.25	5	0.1	0.03	0.05
G3	B3	900	20	719	1.03	5	0	1.8	1.7	0.3	0.55	0.25	0.25	8	0.4	0.03	0.05
G4	B4	900	20	700	1.01	5	0	1.8	1.7	0.3	0.55	0.25	0.25	8	0.4	0.03	0.05

TABLE B.3: Transformer Parameter K2A

Name	From	To	Sn[MV A]	V1[kV]	V2[kV]	R [Ω]	X [Ω]
T1	B1	B5	900	20	230	0	0.15
T2	B2	B6	900	20	230	0	0.15
T3	B3	B11	900	20	230	0	0.15
T4	B4	B10	900	20	230	0	0.15

TABLE B.4: Load Parameter K2A

Name	Bus	Vn[kV]	P [MW]	Q [MVAr]	Model
L1	B7	230	967	100	Z
L2	B9	230	1767	100	Z

TABLE B.5: Shunt Parameter K2A

Name	Bus	Vn[kV]	Q [MVAr]	Model
C1	B7	230	200	Z
C2	B9	230	350	Z

B.1.4 Load Parameters K2A

The load data for the Kundur Two Area test network are presented in Table B.4

B.1.5 Shunts Parameter K2A

The shunt impedance data for the Kundur Two Area test network are presented in Table B.5

B.1.6 Governor Parameters K2A

The governor data for the Kundur Two Area test network are presented in Table B.2

B.1.7 AVR Parameter K2A

The AVR data for the Kundur Two Area test network are presented in Table B.7.

Table B.6: Governor Parameter K2A

Gen	Name	R	Dt	Vmin	Vmax	T1	T2	T3
G1	GOV1	0.05	0.02	0	1	0.1	0.09	0.2
G2	GOV2	0.05	0.02	0	1	0.1	0.09	0.2
G3	GOV3	0.05	0.02	0	1	0.1	0.09	0.2
G4	GOV4	0.05	0.02	0	1	0.1	0.09	0.2

Table B.7: AVR Parameter K2A

Gen	Model	K	TA	TB	TE	Emin	Emax
G1	AVR1	100	2	10	0.05	-3	3
G2	AVR2	100	2	10	0.05	-3	3
G3	AVR3	100	2	10	0.05	-3	3
G4	AVR4	100	2	10	0.05	-3	3

Table B.8: PSS Parameter K2A

Gen	Model	K	T	T1	T2	T3	T4	Hlim
G1	PSS1	50	10	0.5	0.5	0.05	0.05	0.03
G2	PSS2	50	10	0.5	0.5	0.05	0.05	0.03
G3	PSS3	50	10	0.5	0.5	0.05	0.05	0.03
G4	PSS4	50	10	0.5	0.5	0.05	0.05	0.03

Table B.9: Dynamic Load Parameter K2A

Name	Bus	nps	npt	Tp	P0
Load5	B5	0	2	3	1
Load6	B6	0	2	3	1
Load7	B7	0	2	3	1
Load8	B8	0	2	3	1
Load9	B9	0	2	3	1
Load10	B10	0	2	3	1
Load11	B11	0	2	3	1

B.1.8 PSS Parameters K2A

The PSS data for the Kundur Two Area test network are presented in Table B.8.

B.1.9 Dynamic Load Model Parameters K2A

The dynamic load model data for the Kundur Two Area test network are presented in Table B.9

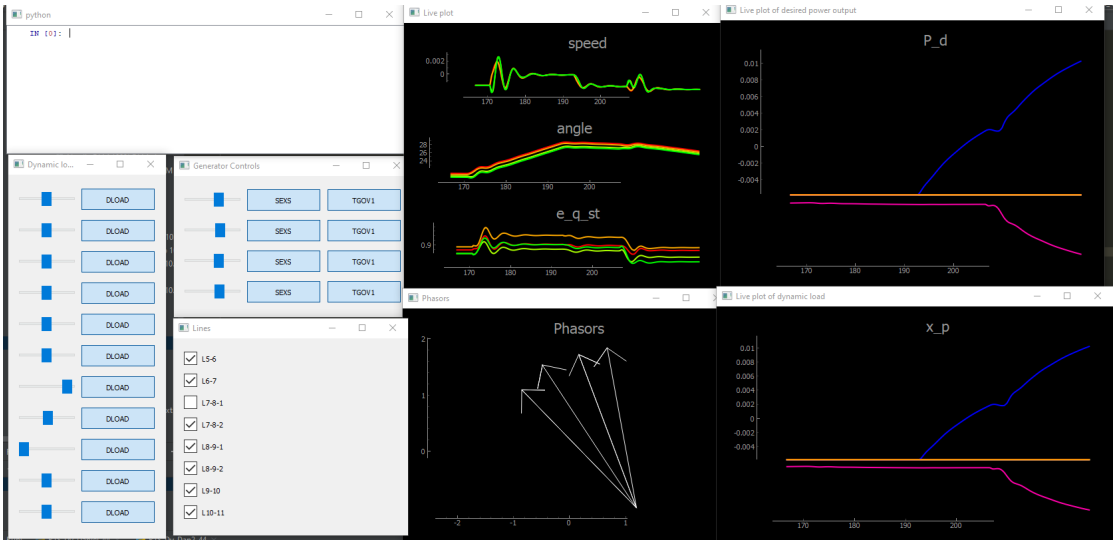

FIGURE B.1: Real-time simulation of time series to stabilized the system manually by injection or extraction of dynamic load model control button.

Bibliography

[1] D. Karlsson and D.J. Hill. Modelling and identification of nonlinear dynamic loads in power systems. *IEEE Transactions on Power Systems*, 9(1):157–166, 1994. doi: 10.1109/59.317546.

[2] Jan Machowski, Zbigniew Lubośny, Janusz W. Bialek, and James R. Bumby. Power system dynamics. stability and control. 3rd edition. 2020.

[3] Horia Andrei, Paul Cristian Andrei, Luminita M. Constantinescu, Robert Beloiu, Emil Cazacu, and Marilena Stanculescu. *Electrical Power Systems*, pages 3–47. Springer International Publishing, Cham, 2017. ISBN 978-3-319-51118-4. doi: 10.1007/978-3-319-51118-4_1. URL https://doi.org/10.1007/978-3-319-51118-4_1.

[4] Adriel Pérez Tellez. Modelling aggregate loads in power systems. 2017.

[5] NordREG. Nordic energy regulation power though cooperation. 2019.

[6] Daniel Weldai. Future operation and control of power systems -laboratory models and real time simulation. 2021.

[7] Abdulrasaq Gbadamosi. Dynamic load modelling in real time digital simulator (rtds). 2017.

[8] Jef Beerten, Oriol Gomis-Bellmunt, Xavier Guillaud, Johan Rimez, Arjen van der Meer, and Dirk Van Hertem. Modeling and control of hvdc grids: A key challenge for the future power system. In *2014 Power Systems Computation Conference*, pages 1–21, 2014. doi: 10.1109/PSCC.2014.7038505. URL https://www.researchgate.net/publication/266259118_Modeling_and_control_of_HVDC_grids_A_key_challenge_for_the_future_power_system.

[9] Takahashi K Sekine, Y and T Sakaguchi. Real-time simulation of power system dynamics.

[10] Yasuji Sekine, K. Takahashi, and Toshiaki Sakaguchi. Real-time simulation of power system dynamics. *International Journal of Electrical Power & Energy Systems*, 16: 145–156, 1994.

[11] M El-Shimy, N Mostafa, AN Afandi, AM Sharaf, and Mahmoud A Attia. Impact of load models on the static and dynamic performances of grid-connected wind power plants: A comparative analysis. *Mathematics and Computers in Simulation*, 149: 91–108, 2018.

[12] Statnett. The way forward –solutions for a changing nordic power system. March, 2018.

[13] L. Bird, M. Milligan, and D. Lew. Integrating variable renewable energy: Challenges and solutions. doi: 10.2172/1097911. URL https://www.osti.gov/biblio/1097911.

[14] P.Venne Student Member IEEE J.Belanger, Member and IEEE J.-N.Paquin, Member. The what, where and why of real-time simulation. page 13, 2000.

[15] P. M. Menghal and A. Jaya Laxmi. Real time simulation: A novel approach in engineering education. In *2011 3rd International Conference on Electronics Computer Technology*, volume 1, pages 215–219, 2011. doi: 10.1109/ICECTECH.2011.5941592.

[16] J Belanger X. Unbehauen R C.Dufour, C.Andrade. Real-time simulation technologies in education: a link to modern engineering methods and practices.

[17] Subrina Noureen, Nimat Shamim, Vishwajit Roy, and Stephen Bayne. Real-time digital simulators: A comprehensive study on system overview, application, and importance. *International Journal of Research and Engineering*, pages 266—-277, 2017.

[18] R. Kuffel, J. Giesbrecht, T. Maguire, R.P. Wierckx, and P. McLaren. Rtds-a fully digital power system simulator operating in real time. In *Proceedings 1995 International Conference on Energy Management and Power Delivery EMPD '95*, volume 2, pages 498–503 vol.2, 1995. doi: 10.1109/EMPD.1995.500778.

[19] P. M. Menghal and A. Jaya Laxmi. Real time simulation: Recent progress amp; challenges. In *2012 International Conference on Power, Signals, Controls and Computation*, pages 1–6, 2012. doi: 10.1109/EPSCICON.2012.6175278.

[20] Z. Fengl, X. Liao, and R. Unbehauen.

[21] M. D. Omar Faruque, Thomas Strasser, Georg Lauss, Vahid Jalili-Marandi, Paul Forsyth, Christian Dufour, Venkata Dinavahi, Antonello Monti, Panos Kotsampopoulos, Juan A. Martinez, Kai Strunz, Maryam Saeedifard, Xiaoyu Wang, David Shearer, and Mario Paolone. Real-time simulation technologies for power systems design, testing, and analysis. *IEEE Power and Energy Technology Systems Journal*, 2(2):63–73, 2015. doi: 10.1109/JPETS.2015.2427370.

[22] R. Razzaghi, M. Paolone, and F. Rachidi. A general purpose fpga-based real-time simulator for power systems applications. In *IEEE PES ISGT Europe 2013*, pages 1–5, 2013. doi: 10.1109/ISGTEurope.2013.6695318.

[23] K.H. Low, Heng Wang, and M.Y. Wang. On the development of a real time control system by using xpc target: solution to robotic system control. In *IEEE International Conference on Automation Science and Engineering, 2005.*, pages 345–350, 2005. doi: 10.1109/COASE.2005.1506793.

[24] Yuan Chen and Venkata Dinavahi. Fpga-based real-time emtp. *IEEE Transactions on Power Delivery*, 24(2):892–902, 2009. doi: 10.1109/TPWRD.2008.923392.

[25] P. Forsyth, T. Maguire, and R. Kuffel. Real time digital simulation for control and protection system testing. In *2004 IEEE 35th Annual Power Electronics Specialists Conference (IEEE Cat. No.04CH37551)*, volume 1, pages 329–335 Vol.1, 2004. doi: 10.1109/PESC.2004.1355765.

[26] D. Brandt, R. Wachal, R. Valiquette, and R. Wierckx. Closed loop testing of a joint var controller using a digital real-time simulator. *IEEE Transactions on Power Systems*, 6(3):1140–1146, 1991. doi: 10.1109/59.119258.

[27] M. Kahrs and C. Zimmer. Digital signal processing in a real-time propagation simulator. *IEEE Transactions on Instrumentation and Measurement*, 55(1):197–205, 2006. doi: 10.1109/TIM.2005.861491.

[28] Meng Joo Er, Chang Boon Low, Khuan Holm Nah, Moo Heng Lim, and Shee Yong Ng. Real-time implementation of a dynamic fuzzy neural networks controller for a scara. *Microprocessors and Microsystems*, 26(9):449–461, 2002. ISSN 0141-9331. doi: https://doi.org/10.1016/S0141-9331(02)00069-8. URL https://www.sciencedirect.com/science/article/pii/S0141933102000698.

[29] Wook Hyun Kwon and Seong-Gyu Choi. Real-time distributed software-in-the-loop simulation for distributed control systems. In *Proceedings of the 1999 IEEE International Symposium on Computer Aided Control System Design (Cat. No. 99TH8404)*, pages 115–119. IEEE, 1999.

[30] Xiang Chen, Meranda Salem, Tuhin Das, and Xiaoqun Chen. Real time software-in-the-loop simulation for control performance validation. *Simulation*, 84(8-9):457–471, 2008.

[31] Ravinder Venugopal, Weihua Wang, and Jean Bélanger. Advances in real-time simulation for power distribution systems. In *2011 International Conference on Energy, Automation and Signal*, pages 1–6, 2011. doi: 10.1109/ICEAS.2011.6147153.

[32] O. A. Mohammed, N. Y. Abed, and S.C. Ganu. Real-time simulations of electrical machine drives with hardware-in-the-loop. In *2007 IEEE Power Engineering Society General Meeting*, pages 1–6, 2007. doi: 10.1109/PES.2007.386269.

[33] Peter Palensky, Milo Cvetković, Digvijay Gusain, and Arun Joseph. Digital twins and their use in future power systems. *Digital Twin*, 2021.

[34] Carlos Miskinis.

[35] Anne-Marie Walters. How digital twins will drive innovation in the energy sector. 2019.

[36] Huaming Pan, Zhenlan Dou, Yanxing Cai, Wenzhu Li, Xing Lei, and Dong Han. Digital twin and its application in power system. In *2020 5th International Conference on Power and Renewable Energy (ICPRE)*, pages 21–26, 2020. doi: 10.1109/ICPRE51194.2020.9233278.

[37] Power system stability and control.

[38] D.J. Hill. Nonlinear dynamic load models with recovery for voltage stability studies. *IEEE Transactions on Power Systems*, 8(1):166–176, 1993. doi: 10.1109/59.221270.

[39] Roger Kearsley. Restoration in sweden and experience gained from the blackout of 1983. *IEEE Power Engineering Review*, PER-7(5):48–48, 1987. doi: 10.1109/MPER.1987.5527255.

[40] T. Ohno and S. Imai. The 1987 tokyo blackout. In *2006 IEEE PES Power Systems Conference and Exposition*, pages 314–318, 2006. doi: 10.1109/PSCE.2006.296325.

[41] Mircea Eremia and Mohammad Shahidehpour. *Handbook of electrical power system dynamics: modeling, stability, and control*, volume 92. John Wiley & Sons, 2013.

[42] Leonard L Grigsby. *Power system stability and control*. CRC press, 2007.

[43] I.R. Navarro, O. Samuelsson, and S. Lindahl. Automatic determination of parameters in dynamic load models from normal operation data. In *2003 IEEE Power Engineering Society General Meeting (IEEE Cat. No.03CH37491)*, volume 3, pages 1375–1378 Vol. 3, 2003. doi: 10.1109/PES.2003.1267352.

[44] Alireza Rouhani and Ali Abur. Real-time dynamic parameter estimation for an exponential dynamic load model. *IEEE Transactions on Smart Grid*, 7(3):1530–1536, 2016. doi: 10.1109/TSG.2015.2449904.

[45] Ines Romero. Dynamic load models for power systems-estimation of time-varying parameters during normal operation. 2002.

[46] Yue Zhu. *Power System Load Models and Load Modelling*, pages 19–47. Springer International Publishing, Cham, 2020. ISBN 978-3-030-37786-1. doi: 10.1007/978-3-030-37786-1_2. URL https://doi.org/10.1007/978-3-030-37786-1_2.

[47] Ieee standard for synchrophasor measurements for power systems. *IEEE Std C37.118.1-2011 (Revision of IEEE Std C37.118-2005)*, pages 1–61, 2011. doi: 10.1109/IEEESTD.2011.6111219.

[48] Edmund O. Schweitzer and David E. Whitehead. Real-time power system control using synchrophasors. In *2008 61st Annual Conference for Protective Relay Engineers*, pages 78–88, 2008. doi: 10.1109/CPRE.2008.4515048.

[49] KSK Weranga, Sisil Kumarawadu, and DP Chandima. *Smart metering design and applications*. Springer, 2014.

[50] P. Regulski, D. S. Vilchis-Rodriguez, S. Djurović, and V. Terzija. Estimation of composite load model parameters using an improved particle swarm optimization method. *IEEE Transactions on Power Delivery*, 30(2):553–560, 2015. doi: 10.1109/TPWRD.2014.2301219.

[51] Dobrivoje P. Stojanović, Lidija M. Korunović, and J.V. Milanović. Dynamic load modelling based on measurements in medium voltage distribution network. *Electric Power Systems Research*, 78(2):228–238, 2008. ISSN 0378-7796. doi: https://doi.org/10.1016/j.epsr.2007.02.003. URL https://www.sciencedirect.com/science/article/pii/S0378779607000272.

[52] A. Borghetti, R. Caldon, A. Mari, and C.A. Nucci. On dynamic load models for voltage stability studies. *IEEE Transactions on Power Systems*, 12(1):293–303, 1997. doi: 10.1109/59.574950.

[53] Hallvar Haugdal, Kjetil Uhlen, and Hjörtur Jóhannsson. An open source power system simulator in python for efficient prototyping of wampac applications. In *2021 IEEE Madrid PowerTech*, pages 1–6. IEEE, 2021.

[54] Hallvar Haugdal, Kjetil Uhlen, and Hjörtur Jóhannsson. An open source power system simulator in python for efficient prototyping of wampac applications. In

2021 IEEE Madrid PowerTech, pages 1–6, 2021. doi: 10.1109/PowerTech46648.2021.9494770.

[55] Sigurd Hofsmo Jakobsen, Lester Kalemba, and Espen Hafstad Solvang. The nordic 44 test network. *Online: https://figshare. com/projects/Nordic_44/57905*, 2018.

[56] Meir Klein, Graham J Rogers, and Prabha Kundur. A fundamental study of inter-area oscillations in power systems. *IEEE Transactions on power systems*, 6(3): 914–921, 1991.